SAND2012-8323P

FUEL-ASSEMBLY SHAKER TEST PLAN

Tests for Determining Loads on Used Nuclear Fuel under Normal Conditions of Transport

Fuel Cycle Research & Development

Prepared for
US Department of Energy
UFD Campaign
Paul McConnell
Sandia National Laboratories

September 30, 2012

FCRD-UFD-2012-000341

Sandia National Laboratories

Sandia National Laboratories is a multi-program laboratory managed and operated by Sandia Corporation, a wholly owned subsidiary of Lockheed Martin Corporation, for the U.S. Department of Energy's National Nuclear Security Administration under contract DE-AC04-94AL85000.

FCT Quality Assurance Program Document

Appendix E
FCT Document Cover Sheet

Name/Title of Deliverable/Milestone	Fuel-Assembly Shaker Test. Tests for Determining Loads on Used Nuclear Fuel under Normal Conditions of Transport
Work Package Title and Number	ST Transportation – SNL / FT-12SN081305 (Rev. 1)
Work Package WBS Number	**1.02.08.13**
Responsible Work Package Manager	Paul McConnell
	(Name/Signature) [signature]
Date Submitted	

Quality Rigor Level for Deliverable/Milestone	☒ QRL-3	☐ QRL-2	☐ QRL-1 ☐ Nuclear Data	☐ N/A*

This deliverable was prepared in accordance with Sandia National Laboratories

(Participant/National Laboratory Name)

QA program which meets the requirements of

☒ DOE Order 414.1 ☐ NQA-1-2000

This Deliverable was subjected to:

☒ Technical Review	☐ Peer Review
Technical Review (TR)	**Peer Review (PR)**
Review Documentation Provided	**Review Documentation Provided**
☐ Signed TR Report or,	☐ Signed PR Report or,
☐ Signed TR Concurrence Sheet or,	☐ Signed PR Concurrence Sheet or,
☐ Signature of TR Reviewer(s) below	☐ Signature of PR Reviewer(s) below

Name and Signature of Reviewers

Gregg Flores [signature]

*Note: In some cases there may be a milestone where an item is being fabricated, maintenance is being performed on a facility, or a document is being issued through a formal document control process where it specifically calls out a formal review of the document. In these cases, documentation (e.g., inspection report, maintenance request, work planning package documentation or the documented review of the issued document through the document control process) of the completion of the activity along with the Document Cover Sheet is sufficient to demonstrate achieving the milestone. QRL for such milestones may be also be marked N/A in the work package provided the work package clearly specifies the requirement to use the Document Cover Sheet and provide supporting documentation.

SUMMARY

This report is the Sandia National Laboratories milestone (M3FT-12SN0813055) "Normal transport test report" for the Used Fuel Disposition Campaign Storage and Transportation (ST) Work Package.

This test plan defines a test designed to capture the response of a representative fuel assembly in its representative transportation configuration (i.e., *in-an-assembly-within-a-basket-within-a-cask-tied-to-a-transport-conveyance*) to actual loadings imposed during normal conditions of transport.

The representative assembly planned for the test is a 17x17 pressurized water reactor (PWR) assembly.

The assembly rods to be used for the tests will not be actual irradiated zirconium alloy/UO_2-pellet rods. Surrogate rods shall be selected that have similar mass and stiffness as the actual irradiated rods. Due to the cost and availability, copper B280 alloy tubes filled with lead rods approximately meet the criteria for simulating Zircaloy-4/UO_2-pellet rods. They shall be used for most of the positions within the assembly; Zircaloy-4/Pb rods shall be used for those assembly positions which will be instrumented for the test.

Finite-element modeling before the test shall provide information on which rod locations within the assembly should be instrumented and on which locations on those rods the instrumentation for measuring strains and accelerations should be placed. Finite-element modeling after the simulated normal transport tests will allow an estimate of the response all the rods may experience during normal transport based upon the test data from the surrogate rods. The test data will also allow the finite element model to be benchmarked.

The test results will allow for an analytic assessment of the ability of aged, high burnup cladding to withstand normal transport loads by assessing the strength of the aged, high burnup cladding relative to the stresses imposed on the cladding during normal transport.

CONTENTS

FIGURES

TABLES

ACRONYMS

BWR	Boiling Water Reactor
CFR	Code of Federal Regulations
FAST	Facility for Accelerated Service Testing
IAEA	International Atomic Energy Agency
NEPA	National Environmental Policy Act
NRC	Nuclear Regulatory Commission
PNNL	Pacific Northwest National Laboratory
PWR	Pressurized Water Reactor
QA	Quality Assurance
SNL	Sandia National Laboratories
ST	Storage and Transportation
TRUPACT	Transuranic Package Transporter
TTC	Transportation Technology Center
US	United States

FUEL-ASSEMBLY SHAKER TEST PLAN

Tests for Determining Loads on Used Nuclear Fuel under Normal Conditions of Transport

1 INTRODUCTION

There is an international issue concerning storage and subsequent transportation of used nuclear fuel that requires quantitative knowledge of used nuclear fuel material properties and response to mechanical loadings during transport.

Many countries are in the position of having to store their used nuclear fuel longer than originally expected. For example, the closing of Yucca Mountain in the United States (US) and the German response to Fukushima will result in the need for extended storage times in these countries. Other countries are still in the planning stages for disposition of their used nuclear fuel, but they will also require extended storage times to accommodate deliberations on fuel disposition.

There are legitimate concerns for long-term storage associated with the degradation of material properties over time for the entire storage system: fuel, canister, overpack, and pad. An understanding of how degraded materials affect their safety functions over time is important to licensing these systems past their original design life. In addition, degradation of used nuclear fuel may adversely affect cladding integrity during transport after storage. Of the storage system components mentioned above, fuel clad integrity is the first line of defense for containment of the used nuclear fuel and so there is a high priority for better understanding of how its material properties may degrade over time, and if these degraded properties are sufficient to maintain fuel integrity during transportation.

This test program is designed to better understand fuel response to *normal* conditions of transport loadings and to estimate the ability of used nuclear fuel with degraded properties to withstand these loadings. This will be done with a combination of experimental data collection and numerical analyses. The experimental work will focus on using full-scale test articles that are subjected to realistic normal conditions of transport loadings. The test unit will be appropriately instrumented to capture the data needed to conduct numerical analyses. The numerical analyses will be used to augment the experimental data set to a more comprehensive set of conditions that will enable a better understanding of used nuclear fuel behavior under normal conditions of transport. The numerical analyses shall also provide the means to extend the test results from a specific package and assembly to other package/assembly configurations.

The data from the tests described herein shall also be compared to data to be generated in other Department of Energy Used Nuclear Fuel Disposition Campaign activities that will measure mechanical properties of both high burnup and aged used nuclear fuel. By comparing the loads applied to fuel cladding during normal transportation to the strength of used nuclear fuel, an assessment can be made of the ability of the cladding to withstand post-storage transportation environments (Figure 1).

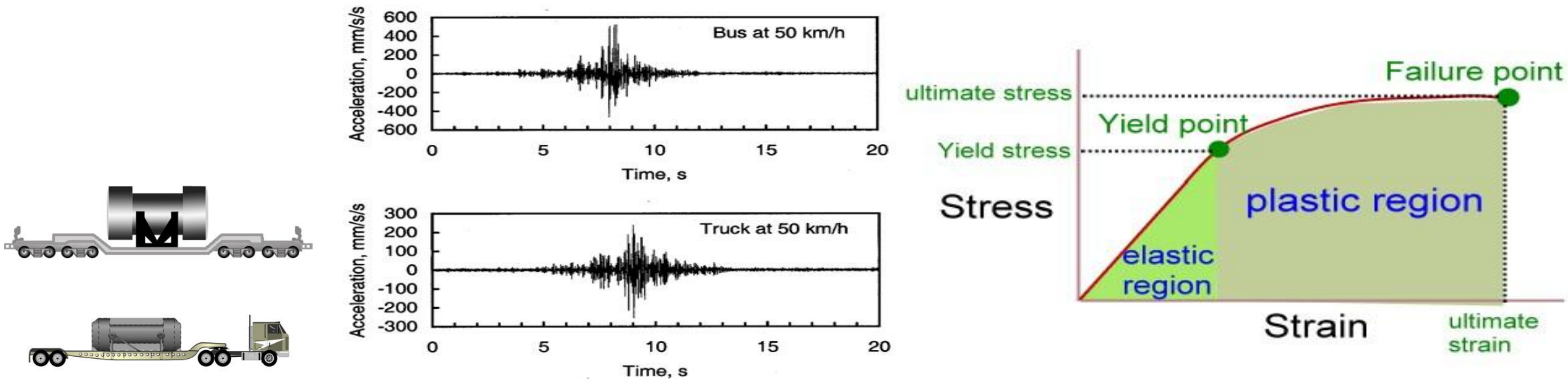

Figure 1. Used nuclear fuel transportation modes, transportation vibration spectra (which result in loads applied to cladding), and material property data.

2 BACKGROUND

2.1 Regulations

US regulations are harmonized with the International Atomic Energy Agency (IAEA) regulations. In the US, the design of casks and performance of the fuel within the casks is governed by 10 CFR Part 71 in the US Code of Federal Regulations. The regulations cover two loading conditions that are important to assure the integrity of used nuclear fuel and are, therefore, important to this test proposal.

- Incident-free transportation: Nuclear fuel must have sufficient strength to sustain its integrity during normal operations. For truck transport, this basically means that the fuel must be strong enough to withstand loadings imposed from driving on roads with various road conditions. For rail, the fuel must be strong enough to withstand loading from over the rail transport as well as longitudinal coupling loads that are imposed. Loading forces and vibrations are the primary loads that need to be obtained for both truck and rail.
- 0.3 meter drop tests: The 0.3 meter drop represents an in-plant accident that may occur while transferring the payload from its storage to its transport configuration. This drop test must be performed (or analyzed) with the package in an orientation that would cause maximum damage.[1] Numerical methods are more easily applied to the analysis of the effects on transport packages and their contents due to a 0.3-meter drop than they are for analysis of the vibrational loading inherent to normal transport conditions.[2]

The loads, to which the used nuclear fuel cladding is subjected during normal conditions of transport, either by truck or by rail, are the result of the induced vibrations and intermittent shock loads. There are virtually no known data for the loads to which used nuclear fuel – the individual pins, the assemblies, the baskets – is subjected during normal transport conditions.

Without mechanical property data for high burnup fuel cladding <u>and</u> knowledge of the loads to which that cladding would experience in a transport environment, predictions of the integrity of the used nuclear fuel during normal transport are speculative and possibly inexact. Mechanical property data for high burnup used nuclear fuel cladding alone is not sufficient for accurate predictions of the behavior of the cladding during normal transport – the applied loads to the cladding during normal transport are also required. Hence this test

---

[1] The regulations are silent regarding the presence of impact limiters on the cask for the 0.3-meter drop. The definition of a transport *package* in 10 CFR 71.4 "means the packaging together with its radioactive contents *as presented for transport*" and "*Packaging* means the assembly of components necessary to ensure compliance with the packaging requirements of this part [and]…*may consist of…devices for…absorbing mechanical shocks*." Furthermore, 10 CFR 71.71(a) Normal Conditions of Transport states that this section is an "[*e*]*valuation of [the] package design*."

[2] A detailed discussion of the US Nuclear Regulatory Commission (NRC) intent regarding the analysis necessary for the drop test may be gleaned from NUREG-1536, Revision 1A, "Standard Review Plan for Used Nuclear Fuel Dry Storage Systems at a General License Facility." But, note that this document addresses used nuclear fuel casks used for dry storage, not transport.

proposal for obtaining load data applied to used nuclear fuel cladding residing within a transport package during normal transport.[3]

2.2 Shock and Vibration

Normal transport loads can be divided into two categories:

- Shock and vibration loading caused by normal over-the-road operations. (A fuel assembly is subjected to cyclic loading conditions as a result of random shock and vibration loading during normal transport conditions.[4])
- The 0.3-m normal regulatory drop event, which is intended to be an initial condition before entering the accident environments.

A large quantity of experimental data has been derived from various sources to quantify the shock and vibration environment of cargo during truck and rail transport. The data usually were collected from instrumentation located at the interface between the packaging or cargo and the transporter, and generally consist of acceleration-response spectra as a function of frequency. The total acceleration response measured for a cargo includes response to superimposed shock and vibration. The vibration component is usually identified as a continuous excitation comprising all responses lower than or equal to 99% of the peaks in the acceleration response records. The remaining higher intensity, infrequently occurring acceleration peaks, correspond to sporadic shock events.

The bounding acceleration shock response spectrum for used nuclear fuel in truck casks for this test program is based on the union of triaxial data (longitudinal, transverse, and vertical axis accelerations) for 20- and 25-tonne cargoes reported in [2-4]. These data are shown in Figure 2. The suggested bilinear curve (in the log-log plane) that bounds these data from above consists of a linearly increasing portion up to a frequency of approximately 3.5 Hz, followed by a constant segment at 4.4-g acceleration, up to a maximum frequency of 300 Hz. For even greater simplicity, the dashed line indicated on the figure could be used at low frequencies, but this may be overly conservative because low-frequency response may be of dominant importance for the fuel assembly system. The data from [2] have been analyzed in a more detailed manner for this test as described in Section 5.

[3] Sandia National Laboratories conducted many tests in the late 1980s – early 1990s to establish the loading on transport packages during normal transport (summarized in a later section). This test campaign measured loading on the external surface of the transport package, not on the contents, which experience a somewhat different loading profile. The methodology for measuring the loads in the previous Sandia National Laboratories program has some analogies to the current test proposal, so pertinent aspects of the previous work can be applied to the current test proposal.

[4] The sensitivity of fuel rod failure due to fatigue was investigated in [1]. Analyses indicate that the magnitudes of the cyclic loads are such that the stresses induced in the cladding are below the endurance limit of the Zircaloy cladding. Even an infinite number of cyclic loads apparently would not propagate existing cracks into fuel rod failures. But, the fatigue strength of high burnup cladding – currently unknown – may require reanalysis of the fatigue issue.

The bounding rail shock spectrum is based on the union of measured triaxial data for a 45-tonne cargo reported by Magnuson [4-5]. The measured data include responses to typical shock generating events, e.g., crossing of bridges and switches, and coupling event shocks.

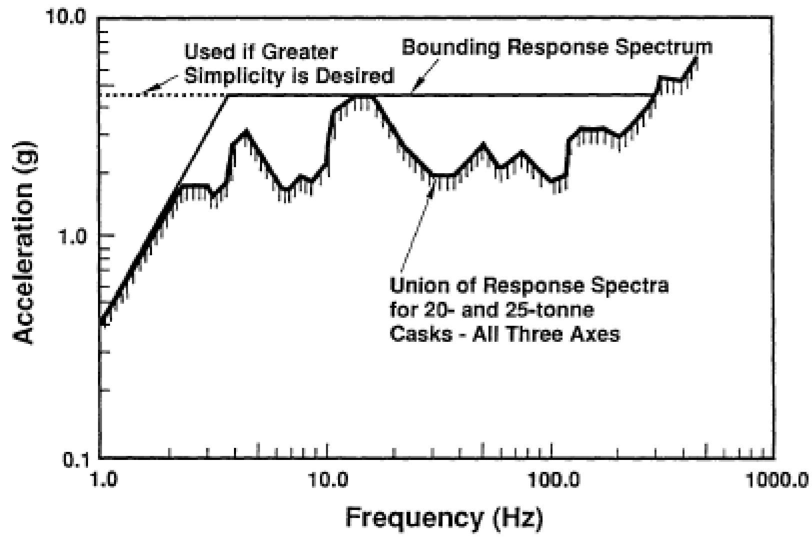

Figure 2. Bounding acceleration shock response spectrum for a truck cask at 3% damping [1].

The bounding truck vibration data for all three response directions are shown in Figure 3.

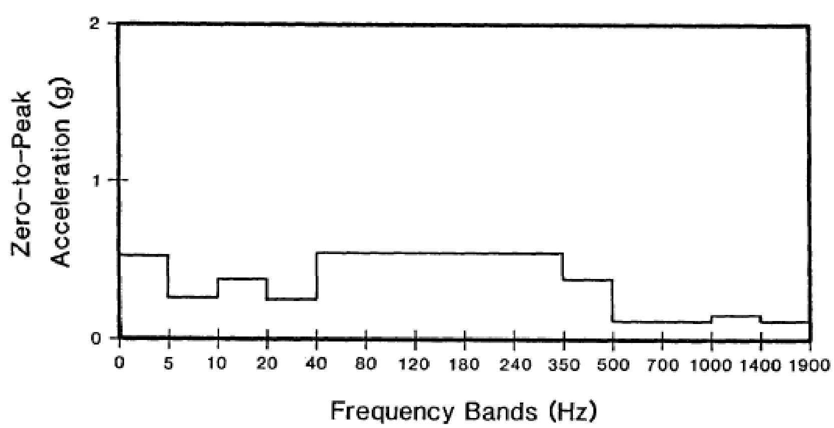

Figure 3. Bounding truck vibration data for all three axes [1].

The analyses in [1] showed that an unirradiated assembly will remain elastic under normal transportation shock and vibration loading conditions. The maximum tensile stress is 155 MPa and occurs at the bottom of the rod adjacent to the end plate. The corresponding maximum spacer grid pinch force is 80.1 N.

3 NORMAL CONDITIONS OF TRANSPORT TEST PLAN

3.1 Introduction

The test is designed to capture the response of used nuclear fuel in its representative configuration to actual loadings imposed during normal conditions of transport. The normal conditions of transport are those defined within the US NRC regulations in 10 Code of Federal Regulations Part 71 [6].

Fuel rods are required to meet conditions defined in 10 CFR Part 71, Subpart F, ¶71.71 during normal transport. In particular, the rods must withstand vibrations and shocks associated with normal transport (while in a transport cask which is tied down to the transport conveyance). NRC guidance is also found in §2.5.6.5 *Vibration* in the "Standard Review Plan for Transportation Packages for Radioactive Material" (US Nuclear Regulatory Commission NUREG-1609 which cites NUREG/CR-2146 and NUREG/CR-0128). [2, 7-8]

To date, licensees have made the technical argument that unirradiated fuel rods and rods irradiated to relatively low burnup levels can withstand the loads imposed upon them by normal transport.

However, fuel is being irradiated to higher burnup levels – which further degrades the cladding – and shall be stored (aged) for longer periods of time. Both of these conditions – high burnup levels and aging during storage – may lead to a situation where the cladding is degraded to such an extent that it may not withstand normal transport loads. There are no data to justify the technical basis for asserting that aged, high burnup fuel can withstand normal transport conditions. The NRC has expressed concerns about approving transport of aged, high burnup fuel without such information.

The data needed to fill this technical gap falls in two categories: 1) the loads imposed directly on rods during normal transport; and 2) the material properties of aged, high burnup cladding. (See Figure 1.)

The goals of this test program are to expand understanding of used nuclear fuel loading environments and subsequent response to these environments. Given a quantitative understanding of fuel rod response, material properties of high burnup, degraded fuel can be coupled with realistic loadings to analytically estimate degraded fuel response to these transport conditions.

The objectives of this test program are to

- Simulate over-the-road tests on a full-scale fuel assembly by applying loadings that used nuclear fuel cladding would experience during normal conditions of transport.
- Instrument the cladding to capture mechanical load, strain, vibration, and shock inputs imposed by the mechanical loadings resulting from the normal condition of transport loading.

3.1.1 Basis of test

The ideal test would be to place an *irradiated* fuel assembly in an actual cask and do over-the-road/rail tests to measure the vibrational loads on the rods. But, doing such a test with an irradiated assembly would be extremely difficult and expensive.

So, an alternative solution is to use an *unirradiated* assembly with surrogate rods (no UO_2 pellets) in an actual cask. However, the only casks available are truck casks and all of those are contaminated on the inside - the casks have all been in pools - a major detriment for performing the tests due to Environmental, Safety, & Health considerations. In addition, the lease price for such a truck cask is significant.

The practical alternative is to place a representative, surrogate fuel assembly on a shaker and subject the assembly to vibrations and shocks simulating normal transport via a truck (or rail) cask. That is the basis of this test plan.

3.1.2 General description of test

This test proposal is designed to capture the response of cladding in its representative configuration (i.e., in-an-assembly-within-a-basket-within-a-cask-tied-to-a-transport-conveyance) to actual loadings imposed during normal conditions of transport. Finite-element modeling after the normal transport tests, coupled with degraded material property data from other UFD experimental work, will allow an estimate of the response irradiated rods would have experienced during the road tests based upon the test data from the surrogate rods.

The assembly planned for the test will represent a 17x17 PWR assembly.

The rods to be used for the tests will not be actual irradiated zirconium-alloy/UO_2-pellet rods. Surrogate rods shall be selected that have similar mass and stiffness as the actual irradiated rods. Copper B280 alloy tubes filled with lead rods approximately meet the criteria for simulating Zircaloy-4/UO_2-pellet rods. They shall be used for most of the positions with the assembly; Zircaloy-4/Pb rods shall be used for those assembly positions which will be instrumented for the test.

Finite-element modeling before the test shall provide information on which rod locations within the assembly should be instrumented and on which locations on those rods the instrumentation for measuring strains and accelerations should be placed. Finite-element modeling after the normal transport tests are conducted will allow an estimate of the response all the rods would have experienced during the road tests based upon the test data from the surrogate rods. The test data will also allow the finite element model to be benchmarked.

The test results will allow for an analytic assessment of the ability of aged, high burnup cladding to withstand normal transport loads by comparing the strength of the aged, high burnup cladding to the stresses imposed on the cladding during normal transport.

This test proposal provides data for the mechanical loads to which fuel rods are subjected during normal transport conditions. The integrity of the cladding is a function of its 1) material properties – yield and tensile strength, elastic modulus, fatigue strength, fracture toughness – all of which may degrade with high burnup and long aging times - and 2) the mechanical loads to which the cladding may be subjected. This test proposal addresses only the latter – the mechanical loads applied to the cladding during normal transport conditions.

3.2 Purpose of Test Plan

This document defines the testing of a 17x17 pressurized water reactor (PWR) assembly (Figure 4) containing surrogate fuel rods placed upon a shaker to simulate vibrational and shock loading associated with a normal transport of an assembly within a truck (or rail) cask on a trailer. This test series will be performed by implementing plans and procedures identified in this document.

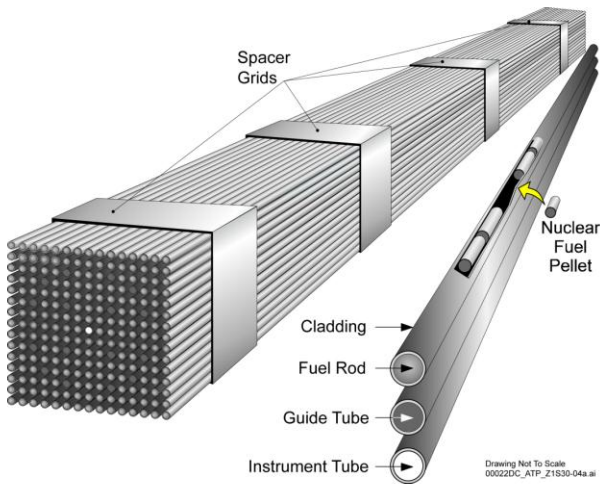

Figure 4. Fuel assembly.

3.3 Test Description

3.3.1 Acquisition of an unirradiated fuel assembly

The most important requirement for the tests is to have available an actual fuel assembly. The assembly could be either PWR or boiling water reactor (BWR).

Both PWR and BWR fuel components have recently been procured by Sandia National Laboratories for an unrelated test program. It is proposed that a PWR assembly be used for the tests described in this plan. PWR fuel is more common than BWR fuel.

Ideally, irradiated, high burnup, aged fuel rods would be used for the tests. Actual fuel, let alone irradiated cladding and fuel, is not an option for the tests, so a surrogate material for the fuel pellets is required.[5] The vibration tests will be conducted with new hollow clad pins (Zircaloy-4 and copper tubing). For the over-the-road test simulation, these pins will be filled with a lead surrogate to represent the mass of the fuel.

The ideal surrogate rod for testing would have the same mass and flexibility as an irradiated rod. Unirradiated fuel has a gap between the fuel pellets and the cladding; irradiated fuel swells closing that gap. Thus, unirradiated fuel rods are not an exact surrogate for irradiated rods. A solid rod of some metal may be appropriate, but a survey indicated that the cost is prohibitive in the lengths necessary to match that of the PWR rods (e.g., thirteen-foot molybdenum rods). It is necessary to attempt to match the properties of surrogate rods with those of irradiated rods, although differences in the rod response can be accounted by numerical analysis post-test. Using estimated properties of irradiated rods allowed selection of a surrogate rod of appropriate stiffness and mass.

[5] The cost is significant – approximately $100k for a 17X17-PWR assembly with Zircaloy rods (sans fuel).

3.3.2 Instrumentation

3.3.2.1 Placement of the instruments on the test unit

Strain gages must be placed on the assembly and cladding to obtain the maximum peak loads to which those components are subjected during normal transport.[6] Triaxial accelerometers will be placed at strategic locations on the assembly and rods. A total of thirty-two to forty-eight channels of data (strain gages plus accelerometers) are reasonable based on experience from previous test programs (the number of gages is to be determined based upon finite element analyses).

Modeling of an assembly will be employed to identify the optimum locations for the instrumentation. But, it is intuitive that placing strain gages on the cladding at the mid-point between spacer grid supports and adjacent to the grids would provide a representative profile of the loading on the rods. The strain gages should be placed on rods at both the top and the bottom of the assembly. Gauges will be placed in such locations along one-half of the length of the assembly.

3.3.2.2 Data reduction and analysis

The protocol for processing the data shall be established using the example of previous test programs at Sandia National Laboratories. The results shall be collated in such a manner as to facilitate future modeling that could estimate loading on other assembly configurations not directly subjected to the transport tests.

The results shall be assessed relative to known or estimated properties of cladding to judge the effect of the normal transport conditions on the integrity of the cladding. Cladding properties of interest, likely available for unirradiated or low burnup conditions, are the yield strength and elastic modulus. The fracture toughness and fatigue strength of cladding, although relevant, are not available.

A LS-DYNA structural model of a detailed 17x17 assembly will be refined and modified at Pacific Northwest National Laboratory (PNNL) to include specific details for the test assembly and basket that will be utilized to impose the loading time history during the actual shaker testing.

Scoping pre-test evaluations will be performed to identify appropriate data collection sites within and about the test assembly. This information will help finalize the test design and provide baseline analyses for future benchmarking and validation of modeling techniques involving LS-DYNA.

A script will be written that converts LS-DYNA fuel assembly specific geometric data and shall port it to Sandia's PRESTO Structural Dynamics code. This tool will help provide baseline analyses for future benchmarking and validation of modeling techniques involving PRESTO as well as cross-comparison between LS-DYNA and PRESTO.

[6] Piezo-electric strain gauges are recommended. Piezo-electric sensors are able to achieve a better resolution than piezo-resistors, while piezo-resistors can be built in much smaller areas. Both types of the strain sensors are capable of high sensitivity measurements, however, and could be used for the tests.

3.3.2.3 Rail Tests

The simulated rail cask tests may be performed at Sandia National Laboratories using vibration and shock inputs from [5].[7]

3.3.3 The 0.3-meter drop test

It is proposed that the 0.3-meter drop test be conducted in a subsequent phase of the test program. The same assembly could be used for the drop tests after the vibrational tests, but not vice versa due to possible damage to the assembly resulting from the drop. It is also proposed that only one cask type, truck or rail, be used for the 0.3-meter drop test.

The 0.3-meter drop represents an accident that may occur while transferring the loaded cask *in its transport configuration* from one position to another, such as, the transfer of the cask from a trailer to a pad. This drop test must be performed (or analyzed) with the package in an orientation that would cause maximum damage.[8,9]

The US regulations are silent regarding the presence of impact limiters on the cask for the 0.3-meter drop. The definition of a transport package in 10 CFR 71.4 is "…the *packaging* together with its radioactive contents as presented for transport" and "*Packaging* means the assembly of components necessary to ensure compliance with the packaging requirements of this part [and]…may consist of…devices for…absorbing mechanical shocks." Furthermore, 10 CFR 71.71(a) Normal Conditions of Transport states that this section is an "[e]valuation of [the] package design." Thus, this test proposal interprets the regulations to allow for the use of "absorbing mechanical shocks" on the cask for the 0.3-meter drop test.

Regardless of whether impact limiters are used for the 0.3-meter drop test, the larger issue is procuring a cask for the test. Owners of existing casks would be reluctant to allow the cask to be dropped, with or without impact limiters. An option is to construct a surrogate cask – a cylinder – into which the fuel assembly can be placed for the drop test.

---

[7] Access to the rail car and transport system (although not a rail cask) may be possible through the US Federal Railroad Administration which has test tracks and has expressed a willingness to participate in such tests. Per the FRA website:

> "There are 48 miles of railroad track available for testing locomotives, vehicles, track components, and signaling devices at the Transportation Technology Center's (TTC) Facility for Accelerated Service Testing (FAST), Pueblo, Colorado. Specialized tracks are used to evaluate vehicle stability, safety, endurance, reliability, and ride comfort. The TTC's tracks eliminate the interferences, delays, and safety issues encountered on an operating rail system (http://www.aar.com/tracks.php)."

[8] Numerical methods are more easily applied to the analysis of the effects on transport packages and their contents due to a 0.3-meter drop than they are for analysis of the vibrational loading inherent to normal transport conditions and they may be an option to an actual drop test.

[9] A detailed discussion of the US NRC intent regarding the analysis necessary for the drop test may be gleaned from NUREG-1536, Revision 1A, "Standard Review Plan for Used nuclear fuel Dry Storage Systems at a General License Facility." But, note that this document addresses used nuclear fuel casks used for dry storage, not transport.

4 SCOPE

This test procedure

- Defines instrumentation requirements
- Defines pre-test and post-test inspection and construction tasks
- Describes steps required to perform the shaker tests
- Identifies applicable supporting and controlling documents
- Defines information, documentation, and data required to document the tests

This procedure, in conjunction with the Sandia National Laboratories (SNL) Job Safety Analysis, Work Control – Level of Rigor, National Environmental Policy Act (NEPA) Review Information, Accept Work, and the Quality Assurance (QA) Program Plan documents, are the planning package for the test program.

Any changes to this procedure will be documented in accordance with the instructions in the SNL Quality Assurance Program Plan.

All supplementary information and test data (calibrations, inspections, change reports, etc.) for this test will be logged and attached to the test results report.

4.1 Test Parameters

The instrumented fuel assembly within its surrogate basket shall be securely affixed upon the shaker. Using the inputs from the analyses of the vibration and shock data from Section 5 the shaker shall impart loads to the assembly and the shaker data acquisition system shall record the responses from the accelerometers on the strain gages attached to the selected fuel rods.

The vibration facility in Excitation Equipment Building 6610 Area III at Sandia National Laboratories supports a wide spectrum of activities for the US Department of Energy Nuclear Weapons Complex. These capabilities provide the versatile and controllable simulation of vibration, acceleration, and shock environments, as well as tailored excitations for the development and validation of analytical models. The facility is used extensively for system level tests of full-scale assemblies or items requiring high vibration levels.

The following Figures 5 – 8 describe the test in more detail.

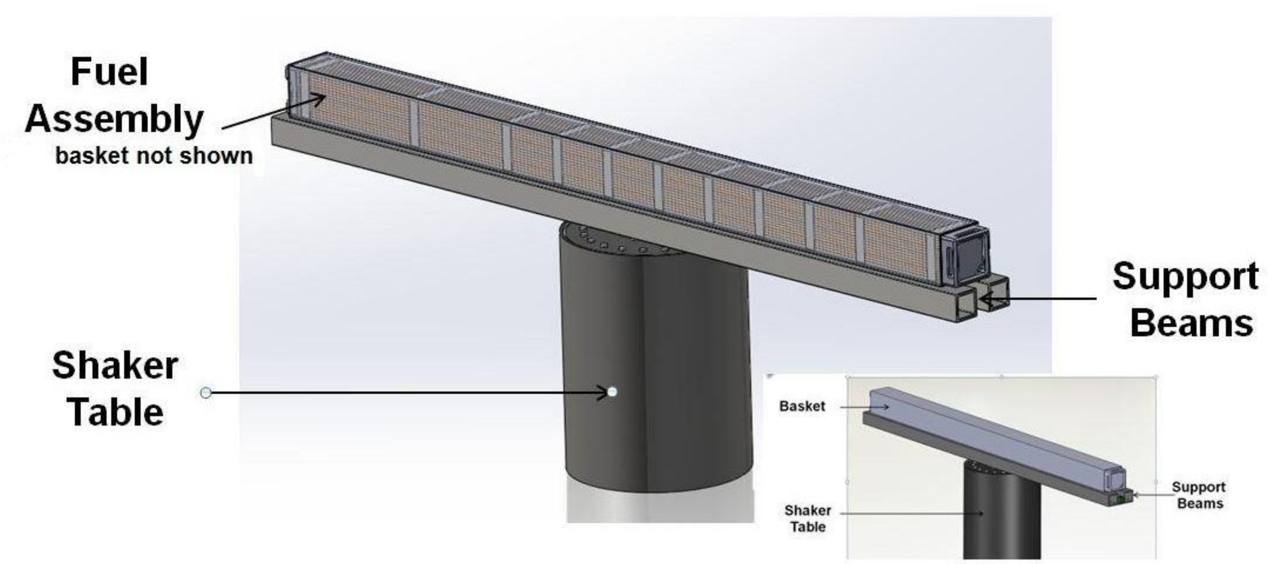

Note: Shaker table not long enough to support enire assembly. Beams used to simulate rigidity of an assembly-within-a-basket-within-a-cask-affixed-to-a-trailer under normal transport conditions.

Figure 5. Placement of assembly with rods, basket, and support beams on shaker.

Experimental Problem	Solution
Actual truck casks too costly (NAC-LWT)	Perform test without a cask Simulate truck transport with shaker table*
Available truck casks are contaminated	
Using UO_2 pellets not feasible	Use Pb rods as surrogate
Availability of Zircaloy tubes limited	Use Cu tubes as surrogate
Surrogates possess material properties dissimilar to Zircaloy	Adjust wall thickness of Cu tubes so that $EI_{Cu} = EI_{Zirc}$ Adjust amount of Pb in tubes to that total assembly weight is that of actual assembly
Assembly is in a basket in a truck cask	Construct basket to NAC-LWT specifications. Place assembly on "stiffeners" to ensure unrealistic bending does not occur about assembly midpoint

*U.S. Nuclear Regulatory Commission, "Shock and Vibration Environments for a Large Shipping Container During Truck Transport (Part II)," NUREG/CR-0128 (SAND Report 78-0337), August 1978.
(Referenced in *Section 2.5.6.5 Vibration* in NUREG-1609, "Standard Review Plan for Transportation Packages for Radioactive Material"

Figure 6. Differences between an actual test in a truck cask and the shaker test.

Zirc and Surrogate Material Properties (Based on equivalent thickness and variable EI)									
Zirc		Aluminum		Brass		Carbon Steel		Copper	
E_{zirc} (GPa)	99	E_{Al} (GPa)	70	E_{Brass} (GPa)	110	E_{SS} (GPa)	205	E_{Cu} (GPa)	115
E_{zirc} (ksi)	14359	E_{Al} (ksi)	10153	E_{Brass} (ksi)	15954	E_{SS} (ksi)	29733	E_{Cu} (ksi)	16679
ρ_{zirc} (g/cm^3)	6.55	ρ_{Al} (g/cm^3)	2.7	ρ_{Brass} (g/cm^3)	8.5	ρ_{SS} (g/cm^3)	7.85	ρ_{Cu} (g/cm^3)	8.94
ρ_{zirc} (g/in^3)	107	ρ_{Al} (g/in^3)	44	ρ_{Brass} (g/in^3)	139	ρ_{SS} (g/in^3)	129	ρ_{Cu} (g/in^3)	147
h (in)	151.79	h (in)	144	h (in)	151.79	h (in)	151.79	h (in)	151.79
Vol_{zirc} (in3)	3.77	Vol_{Al} (in3)	5.38	Vol_{Brass} (in3)	5.67	Vol_{SS} (in3)	5.67	Vol_{Cu} (in3)	5.67
Mass (g)	404.80	Mass (g)	238.19	Mass (g)	790.42	Mass (g)	729.98	Mass (g)	831.34
t (in)	0.0225	t (in)	0.03500	t (in)	0.03500	t (in)	0.03500	t (in)	0.03500
D_{zirc} (in)	0.374	D_{Al} (in)	0.375	D_{Brass} (in)	0.375	D_{SS} (in)	0.375	D_{Cu} (in)	0.375
d_{zirc} (in)	0.329	d_{Al} (in)	0.305	d_{Brass} (in)	0.305	d_{SS} (in)	0.305	d_{Cu} (in)	0.305
EI (k*in2)	5.532	EI (k*in2)	5.543	EI (k*in2)	8.710	EI (k*in2)	16.232	EI (k*in2)	9.106
Zirc Rod (lbs)	0.891	Al Rod (lbs)	0.525	Brass Rod (lbs)	1.739	CS Rod (lbs)	1.606	Cu Rod (lbs)	1.829

$$\text{Moment of Inertia} = I \qquad \frac{\pi(D^4 - d^4)}{64}$$

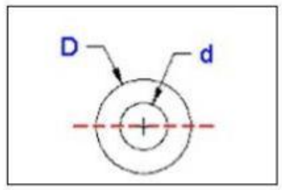

Figure 7. Technical data used to select copper tubes as surrogate rods.

The most important parameter for the test assembly is that its mass be close to the mass of a real assembly. Stiffness of the rods is a secondary but important parameter. This is a non-sequiterA SOLIDWORKS™ simulation predicts a bending response difference of less than 5% between the Cu-Pb rod and Zircaloy-Pb rods.

The combined Modulus / Moment of Inertia properties were checked in order to get an idea on the combined stiffness of each rod:

- EI_{Cu} = 9.106 K-in^2
- EI_{Zirc} = 5.53 K-in^2

The conclusion is that Cu tubing is slightly stiffer than Zircaloy.

Although the material surrogates do not mimic the true material properties exactly, they are the best as far as availability, constructability, and cost. UO_2 and lead share very similar densities but UO_2 is considerably stiffer than Pb. Zircaloy is 30% less dense than copper but Zircaloy shares a similar stiffness with Cu. An actual assembly weighs approximately 1404 lbs. The experimental assembly weighs approximately 1446 lbs. The difference in weight between the actual and experimental assemblies is 42 lbs (3% difference). Although the stiffness of the actual and experimental rods are not the same (mostly due to properties of the UO_2 *v*. Pb), the weights are nearly exact and weight is considered the most important parameter to simulate. Thus, dynamic response of the surrogate test assembly is expected to represent that of a real fuel assembly.

Figure 8 shows the locations of the Zircaloy rods within the assembly (locations are tentative pending finite element analyses).

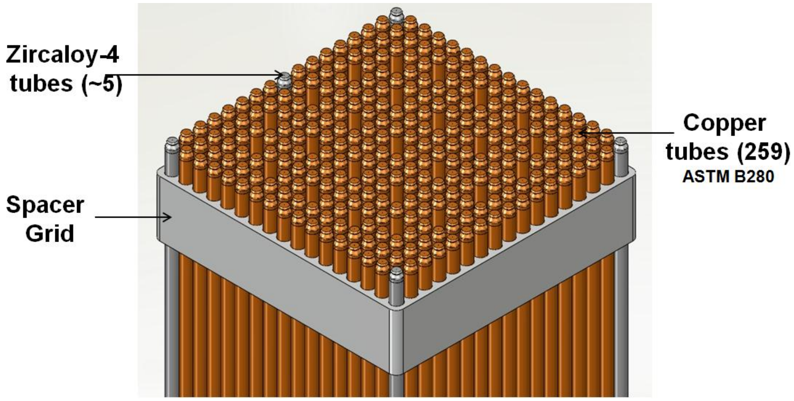

Isometric View of Fuel Rods
(Top Nozzle and Basket not shown)

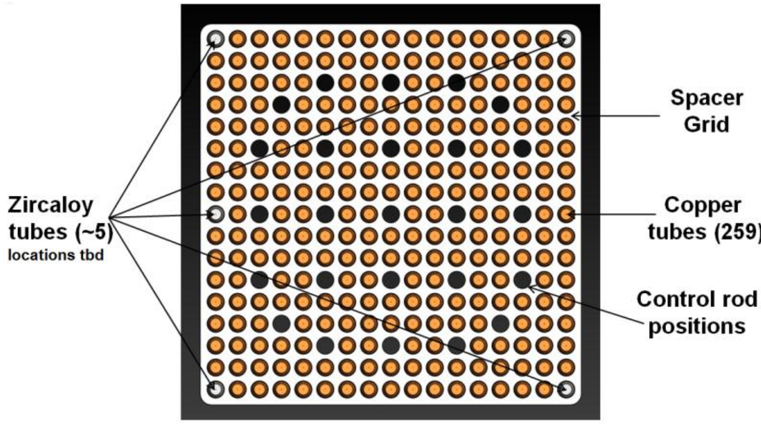

Top View of Assembly

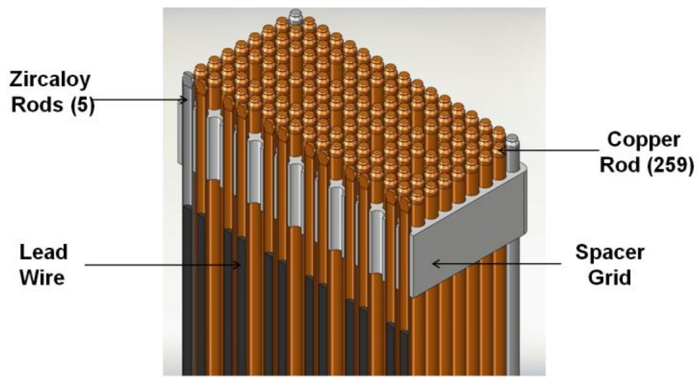

Isometric Section View of Fuel Rods
(Top Nozzle and Basket not shown)

Figure 8. Location of Zircaloy rods within the assembly which will be instrumented.

Input for the shaker table was taken from US Nuclear Regulatory Commission, “Shock and Vibration Environments for a Large Shipping Container During Truck Transport (Part II),” NUREG/CR-0128, August 1978 [2] (referenced in *Section 2.5.6.5 Vibration* in NUREG-1609, “Standard Review Plan for Transportation Packages for Radioactive Material”). Key details from this report are

- Vibration and shock data were measured by accelerometers over a 700 mile journey
- 56,000 lb load for test 1 and 44000 lb for test 2
- Speeds ranged from 0 to 55 mph

Figure 9 shows data from this report.

Using the most conservative data from the 1978 report, the shaker table will simulate the vibration and shock experienced by the cask during transport.

Accelerometers will be placed along the length of the Zircaloy rods in order to measure shock and vertical vibration. Strain gauges will be placed along the length of the rods in order to measure strain. The stress state of the fuel rods will be calculated based on the strain gauge readings.

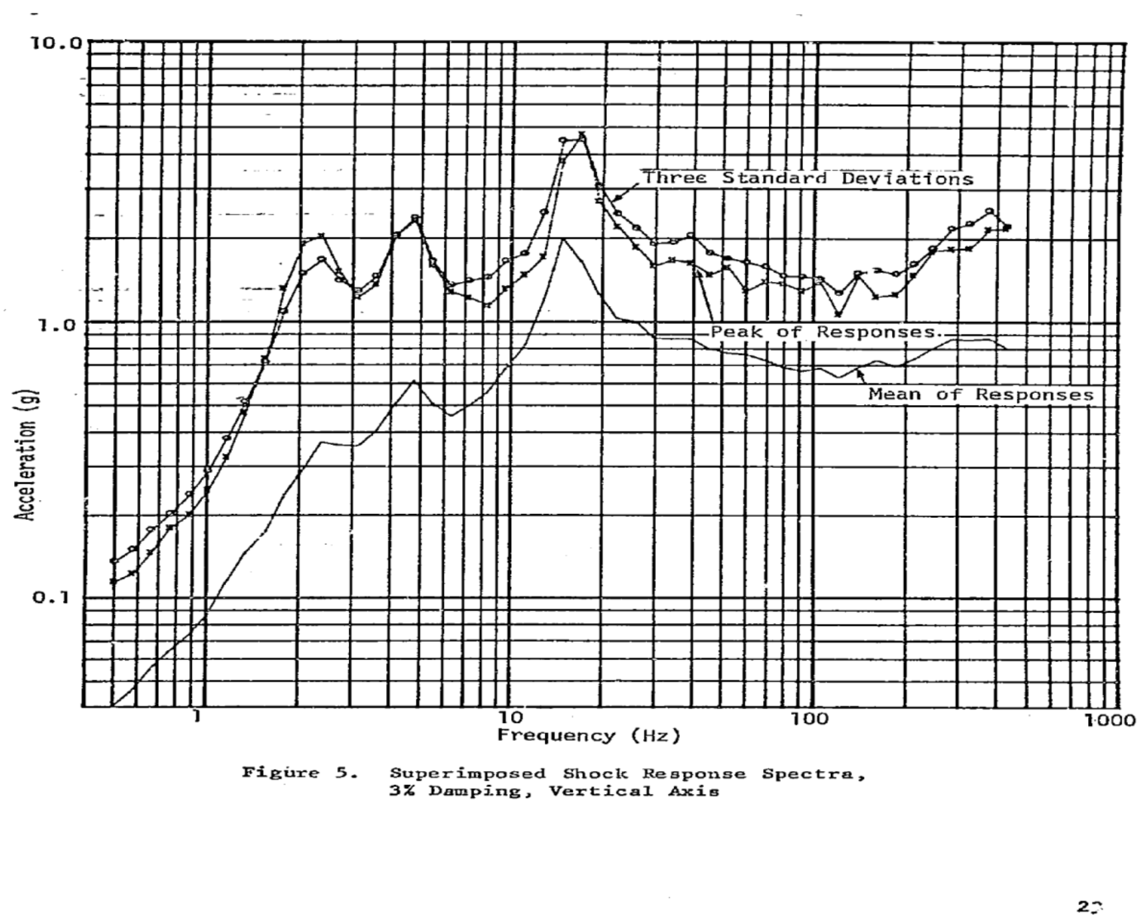

Figure 9. Shock data from the 1978 truck cask transportation report [2].

The following Figure 10 shows data derived from the vibration and shock measured on the truck cask and are the inputs to the shaker as described in Section 5.

Figure 3.0-1: Recommended Random Vibration Test Specification

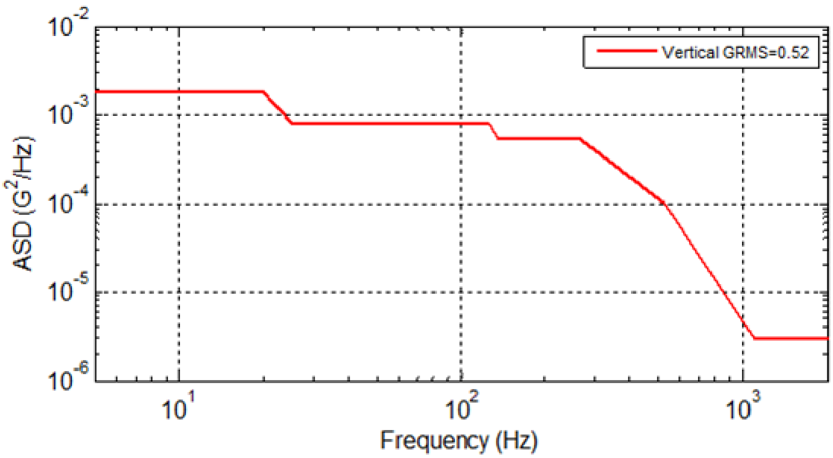

Table 3.0-.1: Vibration Breakpoints

Frequency (HZ)	ASD (G^2/Hz)
5	1.8e-3
20	1.8e-3
25	8.0e-4
125	8.0e-4
135	5.5e-4
265	5.5e-4
530	1.0e-4
1100	3.0e-6
2000	3.0e-6

Figure 4.0-1: Recommended Shock Test Specification

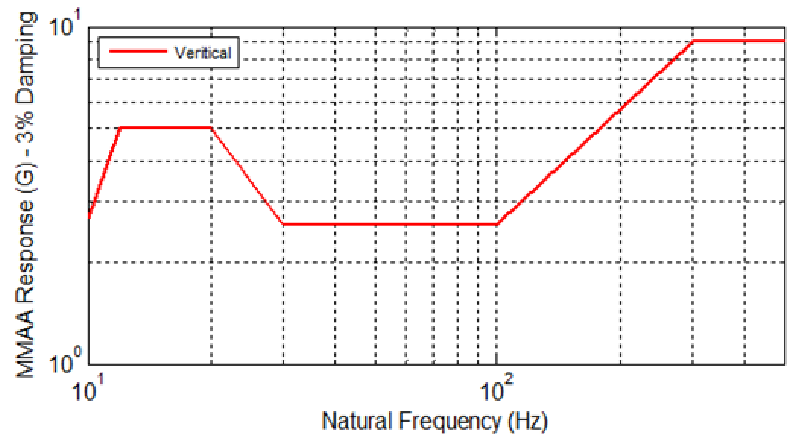

Table 4.0-.1: Reference Shock Breakpoints

Frequency (HZ)	MMAA 3% (G)
10	2.7
12	5.0
20	5.0
30	2.6
100	2.6
300	9.0
600	9.0

Figure 10. Data derived from the truck cask transportation report to be used as input to the shaker.

The following Figures 11 and 12 show the vibration facility and the capabilities of the facility.

4.1.1 Vibration facility

Figure 11. Vibration facility.

4.1.1.1 Vibration facility capabilities

A vertical UD T4000 electrodynamic shaker shall be used for the testing. The system includes

- Control and data acquisition state-of-the-art digital vibration controller
  - 38 input channels available for control, limiting, or real-time monitoring
  - average, maximum, or minimum spectrum control options
- Computer controlled signal conditioning system
  - over 200 channels
  - conditions various types of sensors (e.g., strain gage, force, displacement)
- Data acquisition and analysis system
  - 208 channels
  - 102.4 kilo-samples/s, 24bit resolution
  - data streaming to disk array for long duration recording

Shakers at Sandia used for system level tests of full-scale assemblies or items requiring high vibration levels.

Shown is the Unholtz-Dickie Corporation T4000 electrodynamic shaker for vertical testing

<http://www.udco.com/largetseries.shtml>

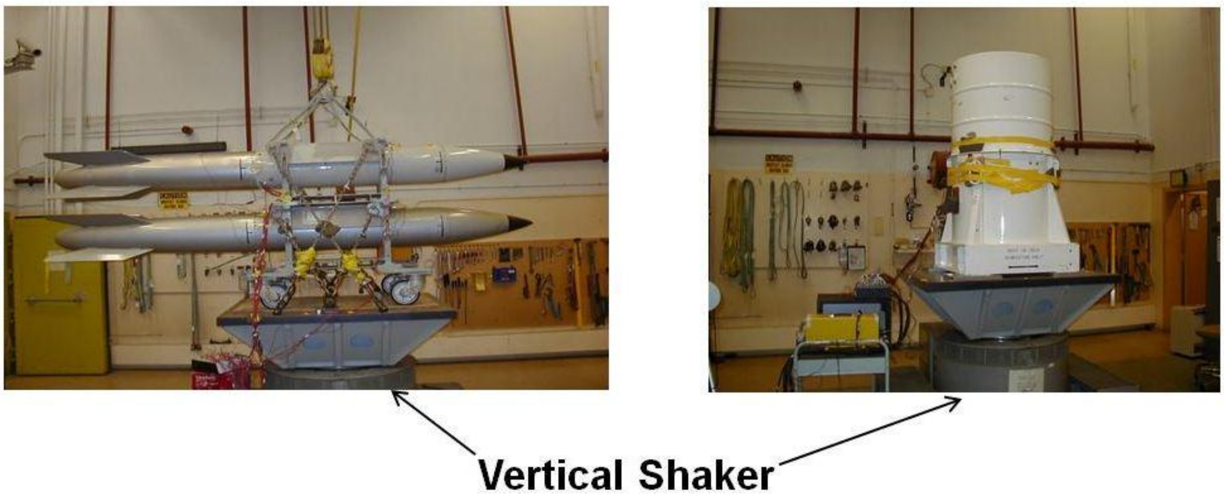

Figure 12. Shaker to be used for test.

The following photograph shows a lead rod inserted in to a copper tube which shall be used as a surrogate Zircaloy/UO_2 rod.

Initial Dimensions for Simulated Copper Fuel Rod Mock-up	
OD (in.)	0.3750
ID (in.)	0.3120
Thickness (in.)	0.0315
Sample Length (in.)	24.0000
Clearance Between Cu & Pb	0.0300

Figure 13. Copper tube containing a lead rod to be used as a surrogate Zircaloy/UO_2 rod.

The following figure shows the dimensions of the simulated basket that will support the assembly on the shaker table (as a basket supports an assembly in a truck cask).

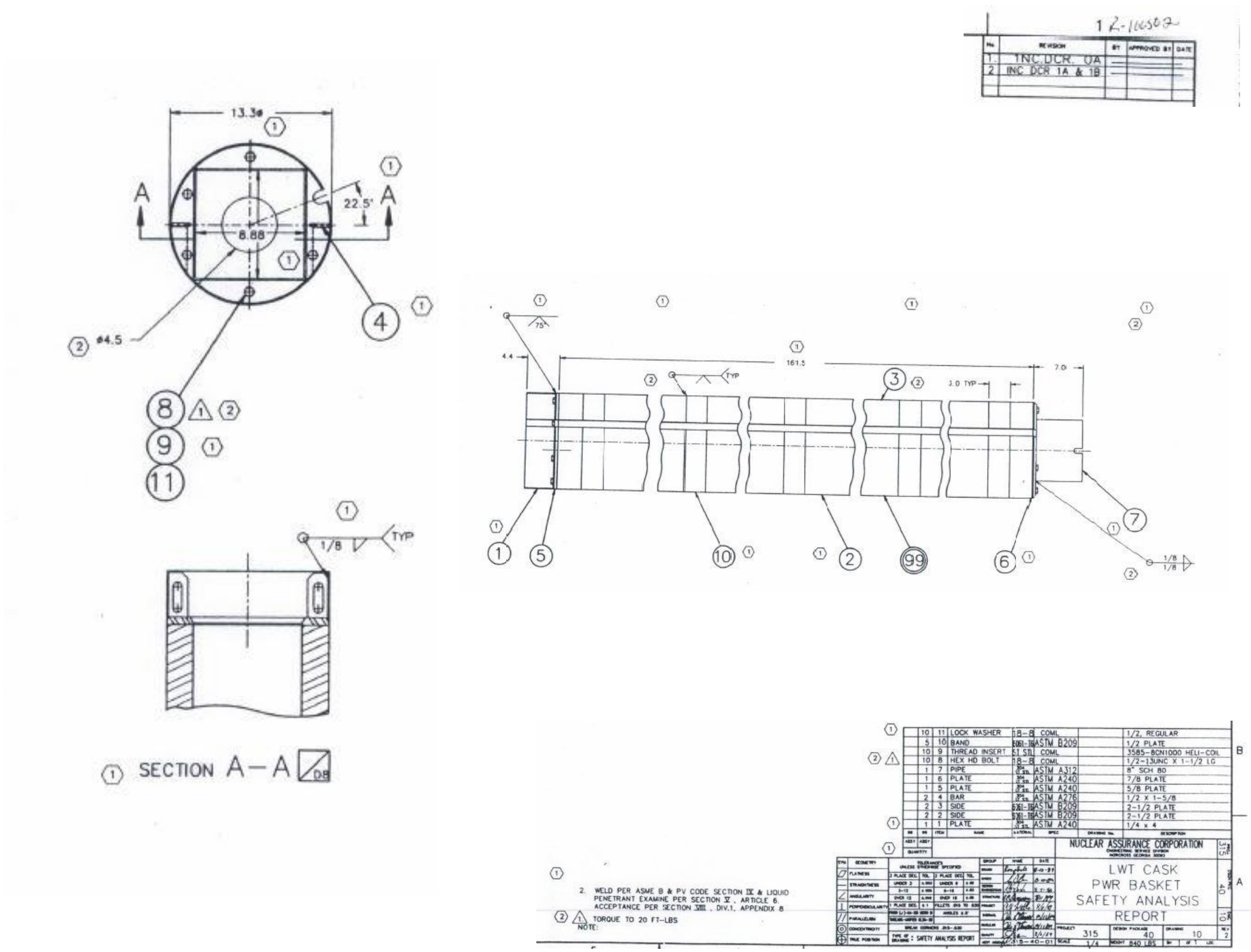

Figure 14. Dimensions of basket to be used to contain the assembly on the shaker (Safety Analysis Report for the NAC-LWT, Revision 27, June 1999, Docket No. 9925 T-88004).

4.2 Instrumentation Installation Tables

Each rod to be instrumented shall have the gauges recorded per the following tables. The strain gages and accelerometers are identified in the figures following the table.

Table 1. Instrumentation Installation Data.
Accelerometers and Strain Gages

Gage ID	Range	Serial Number	Input Resistance (ohms)	Output Resistance (ohms)	Insulation Resistance (ohms)	Field Wire No.	Interface Panel No.	Check OK	Rod Location
A1-1X	20K								
SG1-1X	20K								
A1-2X	20K								
SG1-2X	20K								
A1-3X	20K								
SG1-3X	20K								
A1-4X	20K								
SG1-4X	20K								

ROD #1 (SAME TABLE FOR EACH ROD TO BE INSTRUMENTED)
Accelerometer model #: Model 25 Isotron
Strain gage model #: Vishay Micro-Measurements CEA-03-062UW-350
Installed by ________________________________
Witnessed by ____________________________

GAGE PATTERN DATA

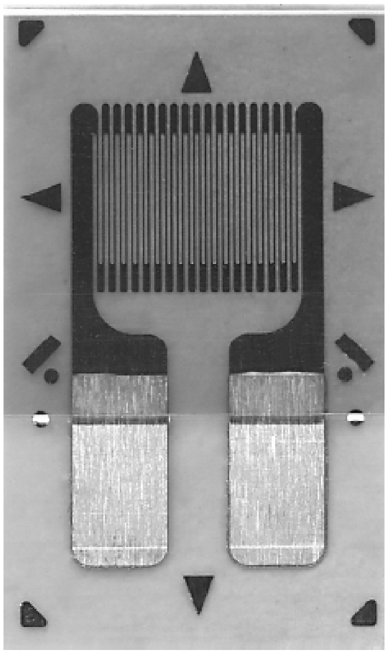

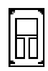

actual size

GAGE DESIGNATION See Note 1	RESISTANCE (OHMS)	OPTIONS AVAILABLE See Note 2
CEA-XX-062UW-120	120 ± 0.3%	**P2**
CEA-XX-062UW-350	350 ± 0.3%	**P2**

DESCRIPTION

General-purpose gage. Exposed solder tab area is 0.07 x 0.04 in [1.8 x 1.0 mm].

GAGE DIMENSIONS Legend: ES = Each Section, S = Section (S1 = Sec 1), CP = Complete Pattern, M = Matrix; inch / millimeter

Gage Length	Overall Length	Grid Width	Overall Width	Matrix Length	Matrix Width
0.062	0.220	0.120	0.120	0.31	0.19
1.57	5.59	3.05	3.05	7.9	4.8

GAGE SERIES DATA

See Gage Series data sheet for complete specifications.

Series	Description	Strain Range	Temperature Range
CEA	Universal general-purpose strain gages.	±3%	−100° to +350°F [−75° to +175°C]

Model 25A Isotron® accelerometer

Features

- World's smallest Isotron®
- Light weight (0.2 gm)
- Flexible cable
- Low impedance output
- Excellent for printed circuit board and disk drive testing

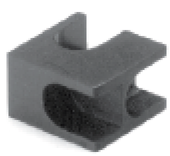

Optional triaxial mounting block

Description

The Endevco® model 25A Isomin™ is an extremely small, adhesive mounted piezoelectric accelerometer with integral electronics, designed specifically for measuring vibration on very small objects. The unit weighs only 0.2 gm, reducing unwanted mass loading effects. The unit comes with two pre-installed fine gage (34 AWG) wires as output leads. These leads can be easily repaired in the field, or a new lead assembly may be reinstalled at the factory. A heavier gage (28 AWG) cable is also provided for extension purpose. The model 25A is ideal for measuring vibration in scaled models, small electronic components, and biomedical research. An optional triaxial mounting block (model 2950M16) is available for setting up three-axis measurement. If a detachable coaxial cable, which can be replaced by the user in the field, is desired, model 25B is available.

The model 25A features Endevco's Piezite® Type sensing element operating in shear mode. The internal electronics inside the accelerometer converts high impedance input into low impedance voltage output through the same cable that supplies the required 4 mA constant current power. Signal ground is isolated from the mounting surface of the unit by a hard anodized surface. A removal tool is included for proper removal in the field.

Endevco signal conditioner models 133, 4416B, 2793, 2776B, 4999, 6634C or Oasis 2000 (4990A-X with cards 428 and/or 433) computer controlled system are recommended for use with this accelerometer.

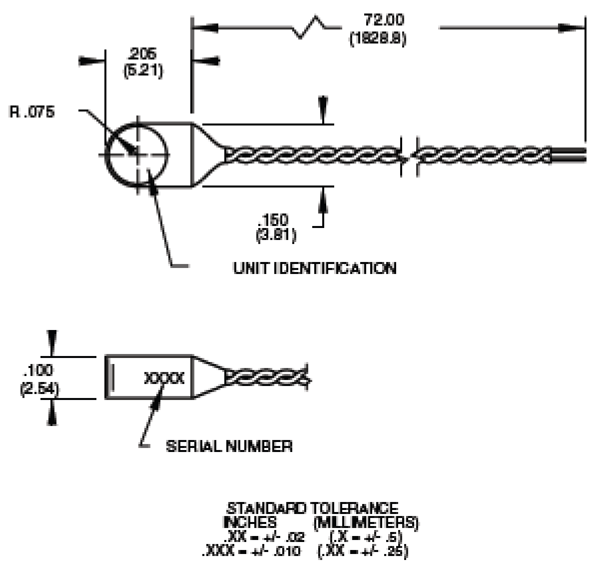

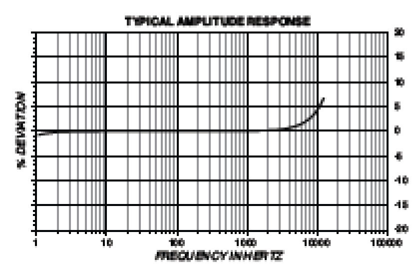

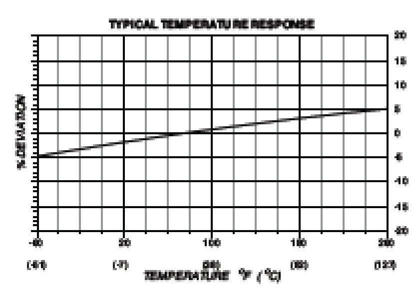

Model 25A
Isotron® accelerometer

MEGGiTT
smart engineering for
extreme environments

Specifications

The following performance specifications conform to ISA-RP-37.2 (1964) and are typical values, referenced at +75˚F (+24˚C), 4 mA and 100 Hz, unless otherwise noted. Calibration data, traceable to National Institute of Standards and Technology (NIST), is supplied.

Dynamic characteristics	Units	
Range	g	±740
Voltage sensitivity		
Typical	mV/g	5
Minimum	mV/g	4
Frequency response		See typical amplitude response
Resonance frequency		
Typical	kHz	50
Minimum	kHz	45
Amplitude response		
±5%	Hz	2 to 8000
±1 dB	Hz	1 to 12 000
Temperature response		See typical curve
Transverse sensitivity	%	≤ 5
Amplitude linearity	%	‹ 2 to full scale

Output characteristics		
Output polarity		Acceleration directed into base of unit produces positive output
DC output bias voltage	Vdc	+8.5 to +11.5
-67°F to +257°F (-55°C to +125°C)	%	±5 typical
Output impedance	Ω	≤ 600
Full scale output voltage	V	±3.7
Residual noise	equiv. g rms	≤ 0.007
Grounding		Signal ground isolated from mounting surface
Load		See load diagram

Power requirement		
Supply current [1]	mA	+3.5 to +4.5
Voltage	Vdc	+18 to +24
Warm-up time	sec	‹ 3

Environmental characteristics		
Temperature range		-67°F to +257°F (-55°C to +125°C)
Humidity		Epoxy sealed, non-hermetic
Sinusoidal vibration limit (survival)	g pk	1000
Shock limit (survival) [2]	g pk	2000
Base strain sensitivity	equiv. g pk/µstrain	0.002
Electromagnetic sensitivity	equiv. g rms/gauss	0.09
Acoustic sensitivity at 140 dB SPL	equiv. g	0.008

Physical characteristics		
Dimensions		See outline drawing
Weight without cable	oz (gm)	0.01 (0.2)
Case material		Aluminum alloy, hard anodized
Mounting [3]		Adhesive

Calibration		
Supplied:		
Sensitivity	mV/g	
Transverse sensitivity	%	
Frequency response	%	20 Hz to 12 kHz

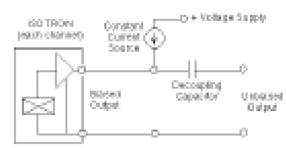

Included accessories

3024-120 (10 ft)	cable assembly, twisted pair [4]
31275	removal tool
32279	mounting wax

Optional accessories

2950M16	triaxial mounting block
133	Signal conditioner
2775B	Signal conditioner
2793	Isotron signal conditioner
4416B	Signal conditioner
4999	Signal conditioner
6634C	Signal conditioner
4990A-X	Oasis 2000 computer-controlled system with cards 428 and/or 433

Notes:

1. Excessive current supply may casue permanent damage to accelerometer.
2. Short duration shock pulses, such as those generated by metal-to-metal impacts, may excite transducer resonance and cause linearity errors. See Tech Paper 290 for more details.
3. Depending on the dynamic and environmental requirements, adhesives such as petro-wax, hot-melt glue, and cyanoacrylate epoxy (super glue) may be used to mount the accelerometer temporarily to the test structure. When removing an epoxy mounted accelerometer, first soften the epoxy with an appropriate solvent, then twist the unit off with the supplied removal tool. Failure to heed this caution may cause permanent damage to the transducer, which is not covered under warranty.
4. Small gage wires are soldered to the terminals at the factory. They are to be spliced together with the supplied cable assembly in the field for extension purpose.
5. Maintain high levels of precision and accuracy using Meggitt's factory calibration services. Call Meggitt's inside sales force at 800-982-6732 for recommended intervals, pricing and turnaround time for these services as well as for quotations on our standard products.

Table 1. Instrumentation Installation Data. (Continued)
Ambient Air Thermocouples

TC ID	TC Type	Serial No.	Loop Resistance (ohms)	Sheath Resistance (ohms)	Location
TC-1 ID TC-1					

Installed by ________________________________
Witnessed by ____________________________
Multimeter:
Manufacturer/Model ____________________________
Serial Number ______________
Calibration Expiration Date ___________

4.3 Vibration Test Procedure

4.3.1 Test preparation

Construct basket by welding four plates of steel per dimensions indicated in Figure 14. Provide cutouts of instrumentation wires.

Insert lead rods into the surrogate copper tubes and the Zircaloy tubes.

Insert all rods into the assembly.

Construct support beams from two square tubes by welding cross-bars along the length of the tubes.

Attach strain gages and accelerometers onto the rods selected for instrumentation.

Complete instrumentation installation forms.

4.3.2 Test set-up

Place support tubes onto shaker. Bolt to shaker.

Place basket/assembly onto support tubes. Bolt to support tubes.

Attach instrumentation from rods, assembly, and shaker surface to the vibration facility recording equipment. Calibrate instrumentation.

Apply vibration input to the shaker.

Apply shock input to the shaker.

Photograph shaker and test unit.

4.3.3 Post-test activities

Disassemble test unit.

Collect test data for post-test analyses.

5 TEST INPUT SPECIFICATIONS: RECOMMENDED VIBRATION AND SHOCK TRANSPORTATION TEST SPECIFICATIONS FOR THE REACTOR FUEL ASSEMBLY[10]

5.1 Introduction

The Environments Engineering Group at SNL was asked to derive a set of set of random vibration and shock test specifications for a laboratory test of a reactor fuel assembly. These specifications were derived from the vibration and shocks presented in references [2,8]. The purpose of the laboratory test is to measure loads during normal highway transportation. This memo presents test specifications for the vertical axis only since it is believed that is the direction which will affect the loading.

At this time the instrumentation has not been optimized and is subject to change. Section 5.2 presents the instrumentation.

Section 5.3 presents the random vibration specification. Section 4 presents the decayed sine specifications.

5.2 Instrumentation

The placement of instrumentation is designed to obtain the peak strain and has not been optimized. Therefore it is subject to change after further discussion with the model group. The accelerometers are used to get insight into what the structure is doing.

Table 2 presents the input accelerometers and their locations. Table 3 presents the response accelerometer and strain gage locations. The first few node shapes will determine where on the tube sections the strain gages are placed. Figure 15 shows the fuel reactor assembly on the shaker table and the input and response locations. Figure 16 shows a cross section of the fuel reactor assembly and the location of Tubes 1 thru 5.

[10] Letter report from Melissa C de Baca to Paul McConnell, April 30, 2012.

Table 2: Response Accelerometers & Strain Gages.

Location	Tube 1	Tube 2	Tube 3	Tube 4	Tube 5
End Spacer	A		A	A	
End Tube Section	A, S	A, S	A, S	A, S	A, S
Mid Span Spacer	A		A	A	
Mid Span Tube Section	A, S	A, S	A, S	A, S	A, S

Note: A – denotes accelerometer; S – denotes strain gage

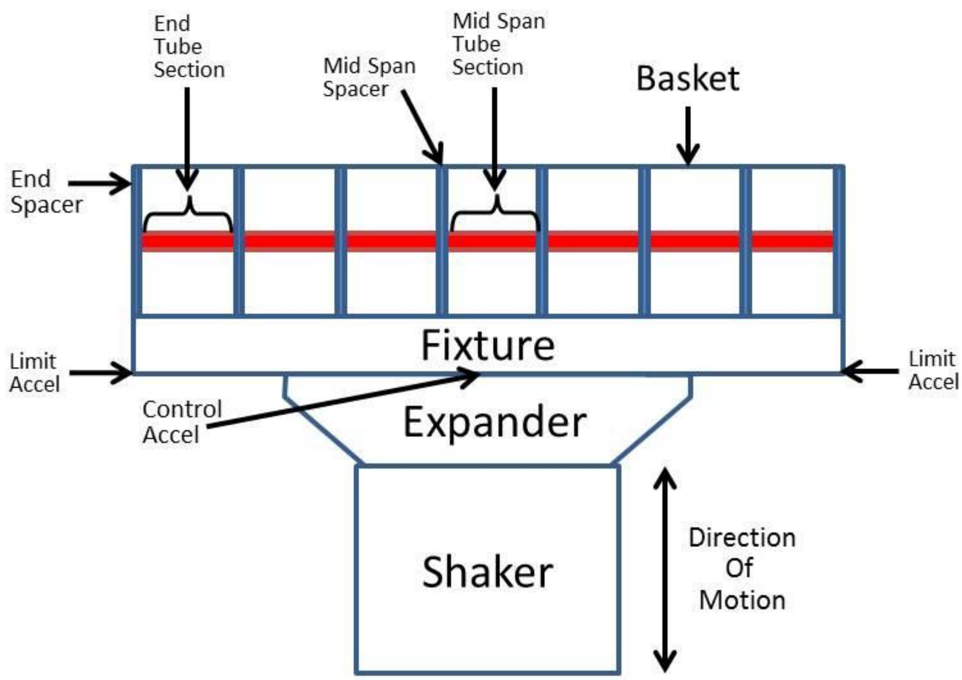

Figure 15. Fuel reactor assembly on shaker table.

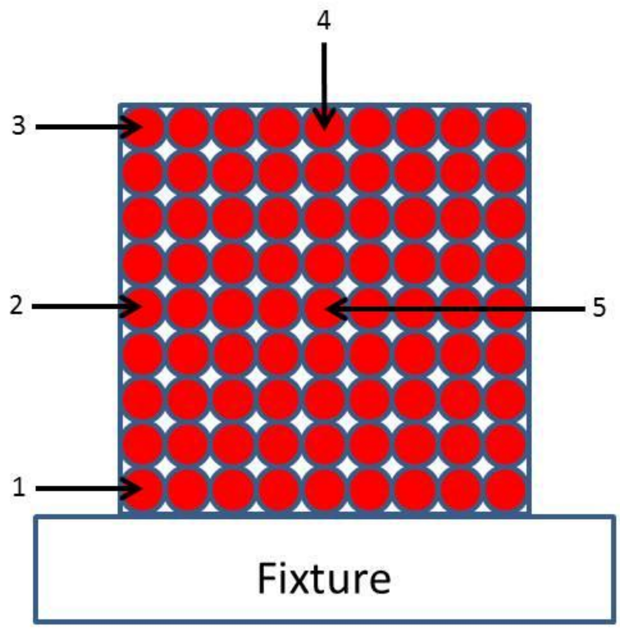

Figure 16. Cross-section of fuel reactor assembly.

5.3 Random Vibration Test Specifications

Figure 17 shows the recommended random vibration test specification to be applied at the midpoint of the fixture. Table 4 presents the corresponding breakpoints. The test should be run for a duration of one minute or long enough to obtain good data. Section 5.5 shows the derivation of this test specification.

We do not know what shape the limit channels should have; therefore they will be a scaled version of the control channel applied at the left and right ends of the fixture. The scaling will be determined at the time of the test.

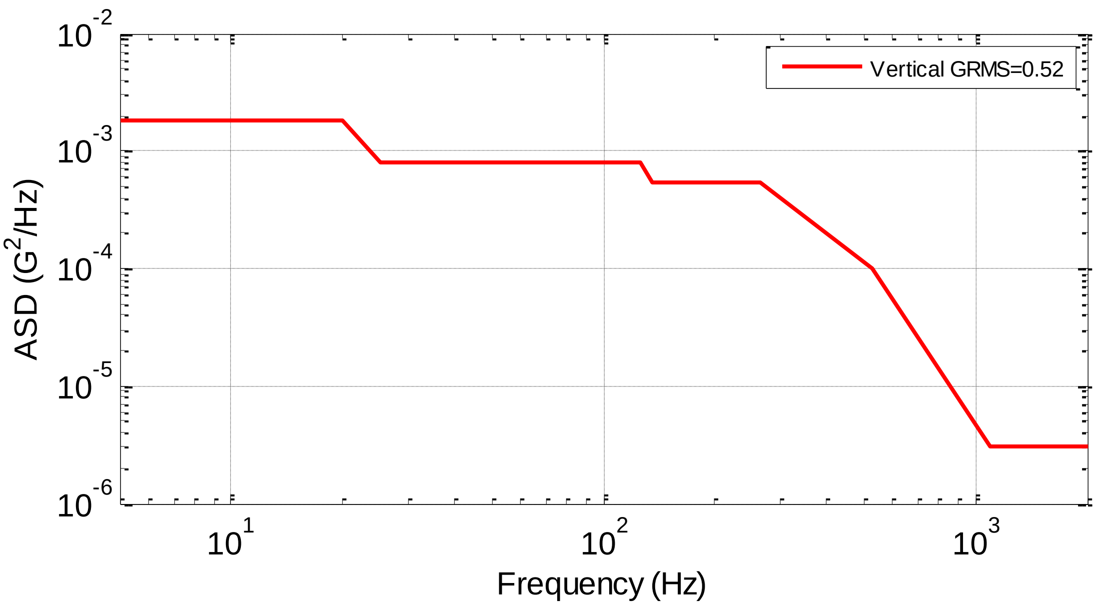

Figure 17. Recommended random vibration test specification.

Table 3: Vibration Breakpoints.

Frequency (HZ)	ASD (G^2/Hz)
5	1.8e-3
20	1.8e-3
25	8.0e-4
125	8.0e-4
135	5.5e-4
265	5.5e-4
530	1.0e-4
1100	3.0e-6
2000	3.0e-6

5.4 Shock – Decayed Sine Specifications and Time Histories

Figure 18 shows the recommended shock test specification. Table 5 lists the corresponding breakpoints. Appendix A shows the derivation of the test specification.

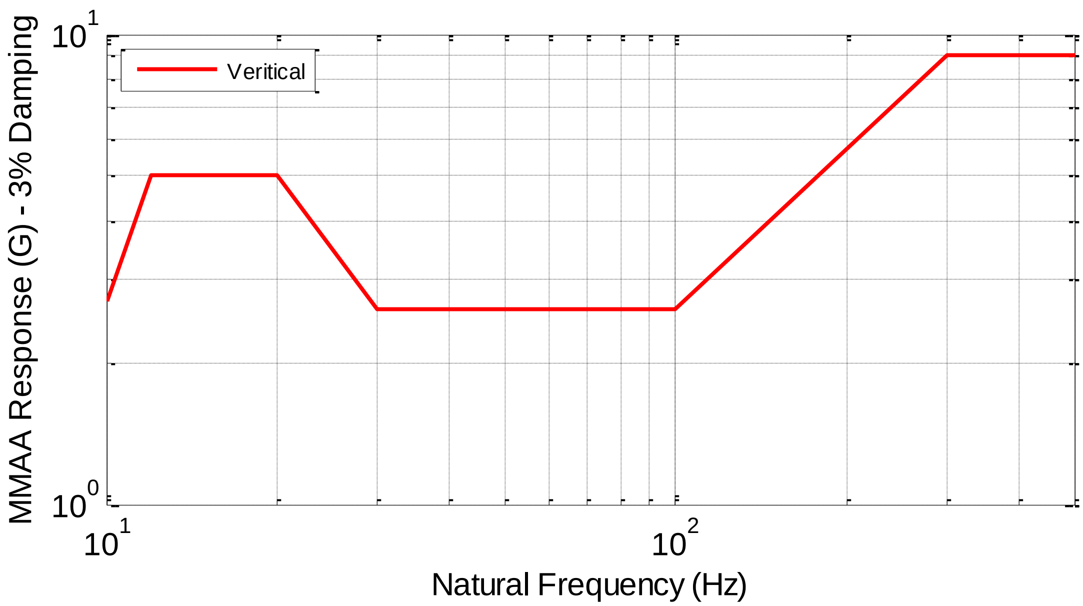

Figure 18. Recommended shock test specification.

Table 4: Reference Shock Breakpoints.

Frequency (HZ)	MMAA 3% (G)
10	2.7
12	5.0
20	5.0
30	2.6
100	2.6
300	9.0
600	9.0

Tables 6 thru 10 list the parameters for the five decayed sine realizations. Shown in these tables are the SRS parameters, the acceleration parameters, and the decayed sine parameters.

Table 5: Initial Realization of Decayed Sine Parameters.

SRS Parameters				
fmin	fmax	pts/oct	Damp	SRS Type
10.00	600.00	8.00	0.03	MMAA

Acceleration History Parameters			
Sample Rate	Frame Size	Gravity Constant	Ptype
5120	8192	386.00	1
Value	Acceleration (G)	Velocity (in/sec)	Displacement (in)
Min	-2.28	-4.51	-0.0530
Max	2.41	4.65	0.0592
Res	-0.18	-0.06	0.0063

Decayed Sine Parameters							
Frequency (Hz)	Accel (G)	Decay Rate	Delay	Frequency (Hz)	Accel (G)	Decay Rate	Delay
10.4	-0.359	0.0286	0.0000	82.6	-0.090	0.0036	0.0000
11.4	0.487	0.0262	0.0000	90.1	0.079	0.0033	0.0000
12.4	-0.440	0.0241	0.0000	98.2	-0.097	0.0030	0.0000
13.5	0.353	0.0221	0.0000	107.0	0.073	0.0028	0.0000
14.7	-0.300	0.0202	0.0000	116.7	-0.124	0.0026	0.0000
16.1	0.265	0.0186	0.0000	127.2	0.114	0.0023	0.0000

17.5	-0.252	0.0170	0.0000	138.6	-0.149	0.0022	0.0000
19.1	0.237	0.0156	0.0000	151.1	0.144	0.0020	0.0000
20.8	-0.218	0.0143	0.0000	164.7	-0.165	0.0018	0.0000
22.7	0.201	0.0132	0.0000	179.5	0.183	0.0017	0.0000
24.7	-0.186	0.0121	0.0000	195.7	-0.193	0.0015	0.0000
26.9	0.120	0.0111	0.0000	213.3	0.219	0.0014	0.0000
29.4	-0.063	0.0102	0.0000	232.5	-0.221	0.0013	0.0000
32.0	0.082	0.0093	0.0000	253.4	0.271	0.0012	0.0000
34.9	-0.122	0.0086	0.0000	276.2	-0.270	0.0011	0.0000
38.0	0.087	0.0078	0.0000	301.1	0.324	0.0010	0.0000
41.5	-0.092	0.0072	0.0000	328.2	-0.294	0.0009	0.0000
45.2	0.114	0.0066	0.0000	357.7	0.283	0.0008	0.0000
49.3	-0.105	0.0061	0.0000	389.9	-0.295	0.0008	0.0000
53.7	0.101	0.0056	0.0000	425.0	0.225	0.0007	0.0000
58.5	-0.067	0.0051	0.0000	463.3	-0.350	0.0006	0.0000
63.8	0.083	0.0047	0.0000	505.0	0.243	0.0006	0.0000
69.5	-0.100	0.0043	0.0000	550.4	-0.259	0.0005	0.0000
75.8	0.093	0.0039	0.0000	600.0	0.393	0.0005	0.0000
				3.5	0.087	0.9500	-0.0457

Table 6: Second Realization of Decayed Sine Parameters.

SRS Parameters				
fmin	fmax	pts/oct	Damp	SRS Type
10.00	600.00	8.00	0.03	MMAA

Acceleration History Parameters			
Sample Rate	Frame Size	Gravity Constant	Ptype
5120	8192	386.00	1
Value	Acceleration (G)	Velocity (in/sec)	Displacement (in)
Min	-2.40	-4.47	-0.0544
Max	2.04	4.25	0.0530
Res	0.01	-0.04	0.0057

Decayed Sine Parameters							
Frequency (Hz)	Accel (G)	Decay Rate	Delay	Frequency (Hz)	Accel (G)	Decay Rate	Delay
10.4	-0.360	0.0286	0.0000	81.5	-0.060	0.0037	0.0000
11.4	0.483	0.0263	0.0000	88.6	0.103	0.0034	0.0000
12.4	-0.496	0.0241	0.0000	96.9	-0.090	0.0031	0.0000
13.4	0.354	0.0223	0.0000	106.8	0.066	0.0028	0.0000
14.8	-0.300	0.0202	0.0000	115.6	-0.168	0.0026	0.0000
16.1	0.300	0.0185	0.0000	130.1	0.109	0.0023	0.0000
17.8	-0.210	0.0168	0.0000	138.2	-0.121	0.0022	0.0000
19.4	0.242	0.0154	0.0000	148.8	0.184	0.0020	0.0000

21.0	-0.242	0.0142	0.0000	168.3	-0.135	0.0018	0.0000
22.6	0.210	0.0132	0.0000	184.1	0.184	0.0016	0.0000
25.1	-0.122	0.0119	0.0000	195.2	-0.206	0.0015	0.0000
27.0	0.147	0.0110	0.0000	209.2	0.207	0.0014	0.0000
29.2	-0.122	0.0102	0.0000	229.8	-0.295	0.0013	0.0000
32.8	0.074	0.0091	0.0000	252.4	0.223	0.0012	0.0000
35.6	-0.119	0.0084	0.0000	277.8	-0.277	0.0011	0.0000
38.2	0.104	0.0078	0.0000	297.6	0.423	0.0010	0.0000
41.8	-0.075	0.0071	0.0000	330.2	-0.244	0.0009	0.0000
45.4	0.061	0.0066	0.0000	362.0	0.243	0.0008	0.0000
48.6	-0.119	0.0061	0.0000	384.7	-0.315	0.0008	0.0000
53.2	0.081	0.0056	0.0000	417.0	0.244	0.0007	0.0000
58.5	-0.100	0.0051	0.0000	458.8	-0.280	0.0007	0.0000
63.0	0.108	0.0047	0.0000	500.7	0.254	0.0006	0.0000
70.9	-0.116	0.0042	0.0000	548.8	-0.320	0.0005	0.0000
74.7	0.096	0.0040	0.0000	574.7	0.358	0.0005	0.0000
				3.5	0.084	0.9500	-0.0457

Table 7: Third Realization of Decayed Sine Parameters.

SRS Parameters				
fmin	fmax	pts/oct	Damp	SRS Type
10.00	600.00	8.00	0.03	MMAA

Acceleration History Parameters			
Sample Rate	Frame Size	Gravity Constant	Ptype
5120	8192	386.00	1
Value	Accel (G)	Velocity (in/sec)	Disp (in)
Min	-2.13	-5.18	-0.0644
Max	2.36	5.06	0.0561
Res	0.03	0.15	-0.0017

Decayed Sine Parameters							
Frequency (Hz)	Accel (G)	Decay Rate	Delay	Frequency (Hz)	Accel (G)	Decay Rate	Delay
10.2	-0.311	0.0292	0.0000	81.0	-0.073	0.0037	0.0000
11.3	0.399	0.0265	0.0000	89.0	0.098	0.0034	0.0000
12.6	-0.675	0.0237	0.0000	97.4	-0.053	0.0031	0.0000
13.2	0.600	0.0226	0.0000	108.1	0.077	0.0028	0.0000
15.1	-0.267	0.0198	0.0000	114.6	-0.138	0.0026	0.0000
16.3	0.300	0.0183	0.0000	128.7	0.116	0.0023	0.0000
17.5	-0.225	0.0170	0.0000	135.9	-0.120	0.0022	0.0000
19.2	0.212	0.0156	0.0000	152.4	0.177	0.0020	0.0000

20.5	-0.246	0.0145	0.0000	164.8	-0.108	0.0018	0.0000
22.7	0.228	0.0132	0.0000	182.3	0.257	0.0016	0.0000
25.3	-0.191	0.0118	0.0000	198.0	-0.167	0.0015	0.0000
27.0	0.136	0.0110	0.0000	217.9	0.191	0.0014	0.0000
29.4	-0.069	0.0101	0.0000	237.4	-0.283	0.0013	0.0000
31.6	0.093	0.0094	0.0000	251.5	0.256	0.0012	0.0000
34.9	-0.107	0.0085	0.0000	279.3	-0.154	0.0011	0.0000
38.3	0.094	0.0078	0.0000	296.6	0.298	0.0010	0.0000
41.9	-0.061	0.0071	0.0000	320.5	-0.393	0.0009	0.0000
45.0	0.114	0.0066	0.0000	362.6	0.323	0.0008	0.0000
49.0	-0.134	0.0061	0.0000	390.3	-0.359	0.0008	0.0000
55.1	0.116	0.0054	0.0000	425.0	0.347	0.0007	0.0000
57.2	-0.070	0.0052	0.0000	473.4	-0.189	0.0006	0.0000
65.1	0.130	0.0046	0.0000	508.3	0.318	0.0006	0.0000
71.1	-0.086	0.0042	0.0000	554.3	-0.262	0.0005	0.0000
77.0	0.082	0.0039	0.0000	574.7	0.281	0.0005	0.0000
				3.4	0.040	0.9500	-0.0466

Table 8: Fourth Realization of Decayed Sine Parameters.

SRS Parameters				
fmin	fmax	pts/oct	Damp	SRS Type
10.00	600.00	8.00	0.03	MMAA

Acceleration History Parameters			
Sample Rate	Frame Size	Gravity Constant	Ptype
5120	8192	386.00	1
Value	Accel (G)	Velocity (in/sec)	Disp (in)
Min	-2.26	-4.52	-0.0492
Max	2.28	4.23	0.0572
Res	-0.03	-0.01	0.0041

Decayed Sine Parameters							
Frequency (Hz)	Accel (G)	Decay Rate	Delay	Frequency (Hz)	Accel (G)	Decay Rate	Delay
10.6	-0.364	0.0281	0.0000	84.7	-0.102	0.0035	0.0000
11.4	0.522	0.0261	0.0000	90.8	0.063	0.0033	0.0000
12.2	-0.535	0.0244	0.0000	99.8	-0.059	0.0030	0.0000
13.4	0.353	0.0223	0.0000	106.9	0.120	0.0028	0.0000
15.0	-0.412	0.0198	0.0000	116.4	-0.114	0.0026	0.0000
15.7	0.405	0.0190	0.0000	129.4	0.107	0.0023	0.0000
17.5	-0.236	0.0170	0.0000	135.7	-0.128	0.0022	0.0000
18.8	0.375	0.0159	0.0000	148.3	0.171	0.0020	0.0000

21.3	-0.239	0.0140	0.0000	162.0	-0.160	0.0018	0.0000
22.9	0.232	0.0130	0.0000	178.7	0.203	0.0017	0.0000
24.7	-0.157	0.0121	0.0000	199.2	-0.208	0.0015	0.0000
26.9	0.153	0.0111	0.0000	216.8	0.237	0.0014	0.0000
28.7	-0.050	0.0104	0.0000	227.4	-0.199	0.0013	0.0000
32.3	0.078	0.0092	0.0000	252.3	0.238	0.0012	0.0000
34.1	-0.103	0.0088	0.0000	276.8	-0.295	0.0011	0.0000
37.2	0.114	0.0080	0.0000	300.1	0.342	0.0010	0.0000
41.5	-0.126	0.0072	0.0000	331.1	-0.308	0.0009	0.0000
44.3	0.074	0.0067	0.0000	360.4	0.281	0.0008	0.0000
50.1	-0.114	0.0060	0.0000	386.1	-0.195	0.0008	0.0000
54.6	0.100	0.0055	0.0000	423.9	0.260	0.0007	0.0000
59.3	-0.114	0.0050	0.0000	452.1	-0.418	0.0007	0.0000
62.7	0.086	0.0048	0.0000	518.1	0.265	0.0006	0.0000
70.2	-0.096	0.0043	0.0000	541.5	-0.170	0.0006	0.0000
76.0	0.081	0.0039	0.0000	574.7	0.350	0.0005	0.0000
				3.5	0.030	0.9500	-0.0449

Table 9: Fifth Realization of Decayed Sine Parameters.

SRS Parameters				
fmin	fmax	pts/oct	Damp	SRS Type
10.00	600.00	8.00	0.03	MMAA

Acceleration History Parameters			
Sample Rate	Frame Size	Gravity Constant	Ptype
5120	8192	386.00	1
Value	Acceleration (G)	Velocity (in/sec)	Displacement (in)
Min	-1.99	-4.91	-0.0592
Max	2.11	5.18	0.0631
Res	-0.04	-0.01	0.0035

Decayed Sine Parameters							
Frequency (Hz)	Accel (G)	Decay Rate	Delay	Frequency (Hz)	Accel (G)	Decay Rate	Delay
10.4	-0.360	0.0287	0.0000	80.7	-0.114	0.0037	0.0000
11.2	0.438	0.0266	0.0000	90.4	0.112	0.0033	0.0000
12.4	-0.508	0.0240	0.0000	100.2	-0.058	0.0030	0.0000
13.4	0.344	0.0222	0.0000	108.1	0.091	0.0028	0.0000
15.1	-0.296	0.0198	0.0000	114.9	-0.094	0.0026	0.0000
16.4	0.464	0.0182	0.0000	126.4	0.136	0.0024	0.0000
17.1	-0.494	0.0174	0.0000	138.4	-0.141	0.0022	0.0000
19.3	0.224	0.0154	0.0000	155.0	0.131	0.0019	0.0000

20.6	-0.197	0.0145	0.0000	161.9	-0.148	0.0018	0.0000
22.6	0.218	0.0132	0.0000	183.0	0.194	0.0016	0.0000
24.8	-0.193	0.0120	0.0000	197.3	-0.185	0.0015	0.0000
27.6	0.127	0.0108	0.0000	212.1	0.167	0.0014	0.0000
29.3	-0.125	0.0102	0.0000	229.0	-0.293	0.0013	0.0000
32.8	0.093	0.0091	0.0000	252.7	0.166	0.0012	0.0000
34.6	-0.059	0.0086	0.0000	276.2	-0.372	0.0011	0.0000
38.5	0.080	0.0078	0.0000	295.4	0.327	0.0010	0.0000
41.9	-0.124	0.0071	0.0000	330.0	-0.307	0.0009	0.0000
45.3	0.111	0.0066	0.0000	353.0	0.297	0.0008	0.0000
49.8	-0.088	0.0060	0.0000	388.0	-0.241	0.0008	0.0000
54.2	0.075	0.0055	0.0000	427.2	0.326	0.0007	0.0000
57.6	-0.086	0.0052	0.0000	457.8	-0.306	0.0007	0.0000
62.6	0.110	0.0048	0.0000	500.0	0.182	0.0006	0.0000
71.4	-0.128	0.0042	0.0000	554.3	-0.266	0.0005	0.0000
74.6	0.077	0.0040	0.0000	574.7	0.329	0.0005	0.0000
				3.5	0.171	0.9500	-0.0459

5.5 Derivation of Test Specifications

The initial plan of the customer was to have a reactor fuel assembly in a large truck cast with the fuel rods instrumented within the cast to measure loads during normal highway transport. The cask was to be placed upon a trailer in a horizontal position for the test. However, procuring a cask was not realistic and plans were made to use the shaker.

The only data available to derive the laboratory test specifications are from two shock and vibration tests for large shipping containers during truck transport performed in the late 70's [2,8]. Section 5.5.1 describes the derivation of the random vibration test specification. Section 5.5.2 describes the derivation of the shock test specification.

5.5.1 Derivation of random vibration test specification

The two documents presented the random vibration data as VIBRAN data which was the 99% level of 0 to peak amplitudes over a frequency band. Table 11 shows the VIBRAN data for the vertical axis.

Table 10: Input to Cargo (g) – Vertical Axis.
99% Level of 0 to Peak Amplitude

Frequency Range	44,000 lb.	56,000 lb.
0 – 5	0.27	0.52
5 – 10	0.19	0.27
10 – 20	0.27	0.37
20 – 40	0.27	0.19
40 – 80	0.52	0.37
80 – 120	0.52	0.37
120 – 180	0.52	0.52
180 – 240	0.52	0.52
240 – 350	0.52	0.52
350 – 500	0.14	0.37
500 – 700	0.07	0.10
700 – 1000	0.07	0.10
1000 – 1400	0.05	0.10
1400 – 1900	0.05	0.10

The first step was to convert the data into an ASD. This is shown in {Eq. A.1-1} where ZPA is the zero to peak amplitude and FR is the frequency band.

$$ASD = (ZPA \div 3)^2 \div \left(FR(2) - FR(1)\right) \qquad \text{\{Eq. A.1-1\}}$$

Once the ASDs were generated the straight line test specification was created. The actual weight of the fuel reactor assembly falls between 44,000 lbs. and 56,000 lbs. therefore it was decided that enveloping the two ASDs would be conservative. Figure 19 shows the recommended test specification and the underlying ASDs.

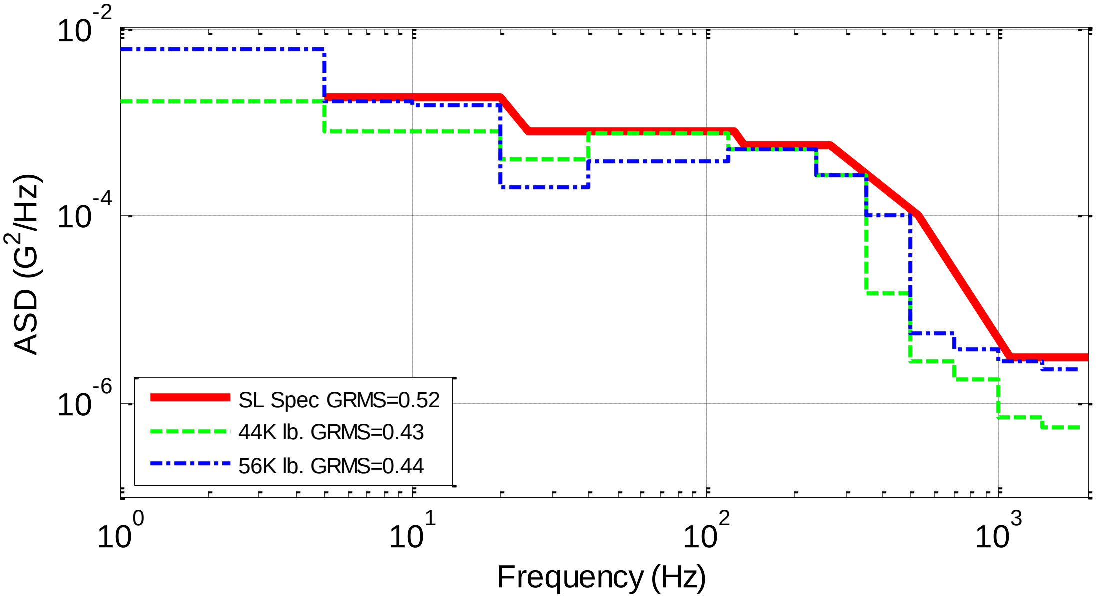

Figure 19. Recommended test specification & underlying ASDs.

5.5.2 Derivation of shock test specification

The shock response spectra were displayed as plots in References 8 and 9. Therefore before being able to use them the data had to be digitized to obtain electronic data. There were three shock responses displayed; the 3σ, the peak of responses, and the mean of responses. Due to the quality of the plot it was decided to envelope the three shock responses when digitizing. Shock response spectra for the 44,000 lb. cargo and the 56,000 lb. cargo were obtained.

The straight line shock test specification was created to envelope the 44,000 lb. shock spectra and the 56,000 lb. shock spectra. Figure 20 shows the recommended test specification and the underlying shock response spectra.

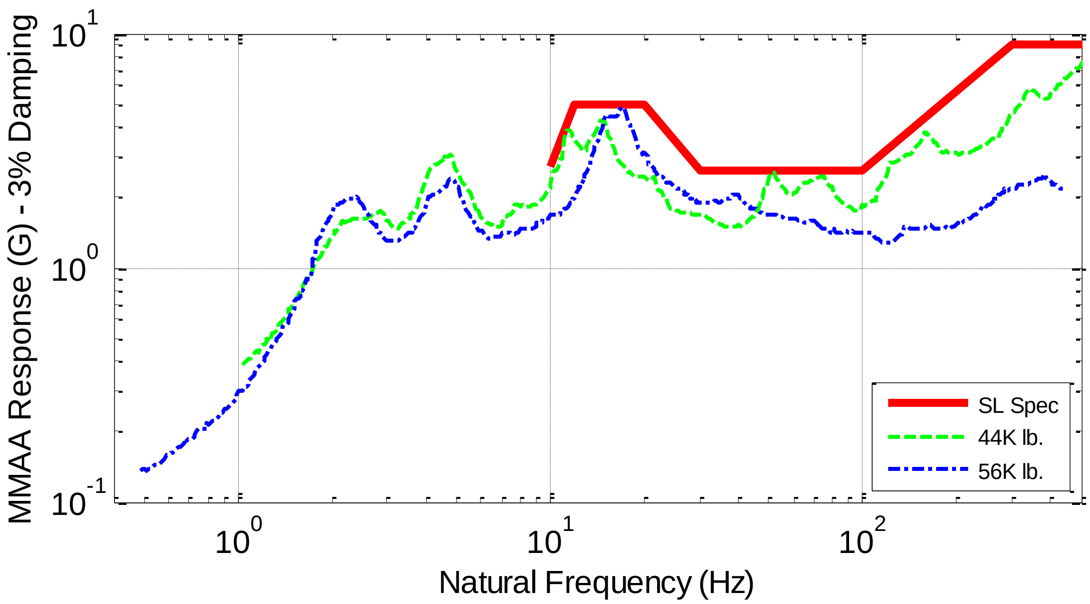

Figure 20. Recommended test specification & underlying shock spectra.

The next step was to obtain the five decayed sine realizations. The transients synthesized are composed of sum of decaying sinusoids which match the specified shock response spectrum. The pulse is compensated for velocity and displacement by adding a delayed decayed sinusoid.

In order to obtain five unique transients, "jitter" was added to the frequencies of the specified shock response spectrums. Figure 21 shows the range a given frequency was allowed to vary. The frequencies were allowed to vary a maximum of 80% from the midpoint (i.e., F_1) in the positive and negative direction (i.e., F_{1low} and F_{1high}). A uniform random distribution was used to determine the amount each frequency varied within its specified range.

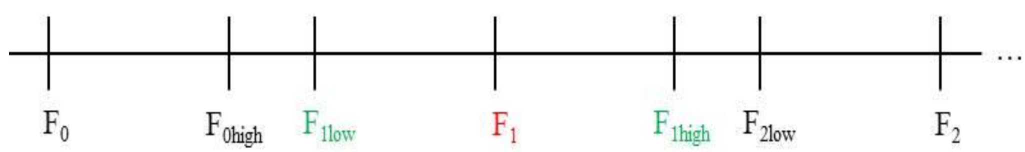

Figure 21. Range of frequencies.

Figures 22 through 26 show the acceleration history, velocity, displacement, and the decayed sine shock spectra versus the reference shock spectra for the five realizations.

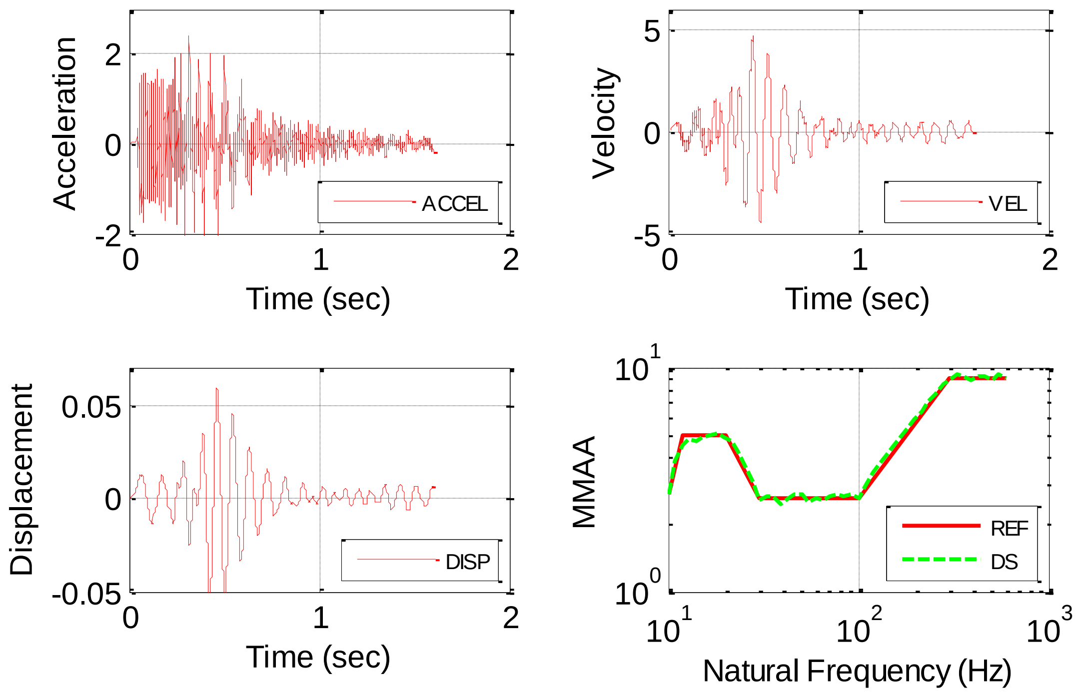

Figure 22. Decayed sine initial realization.

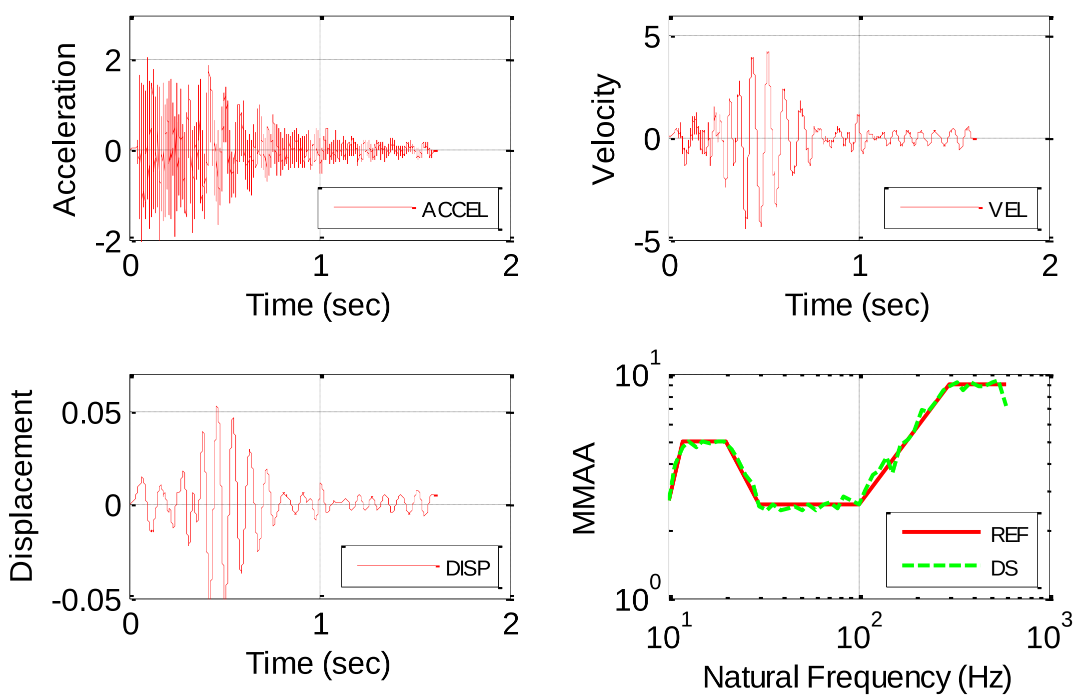

Figure 23. Decayed sine second realization.

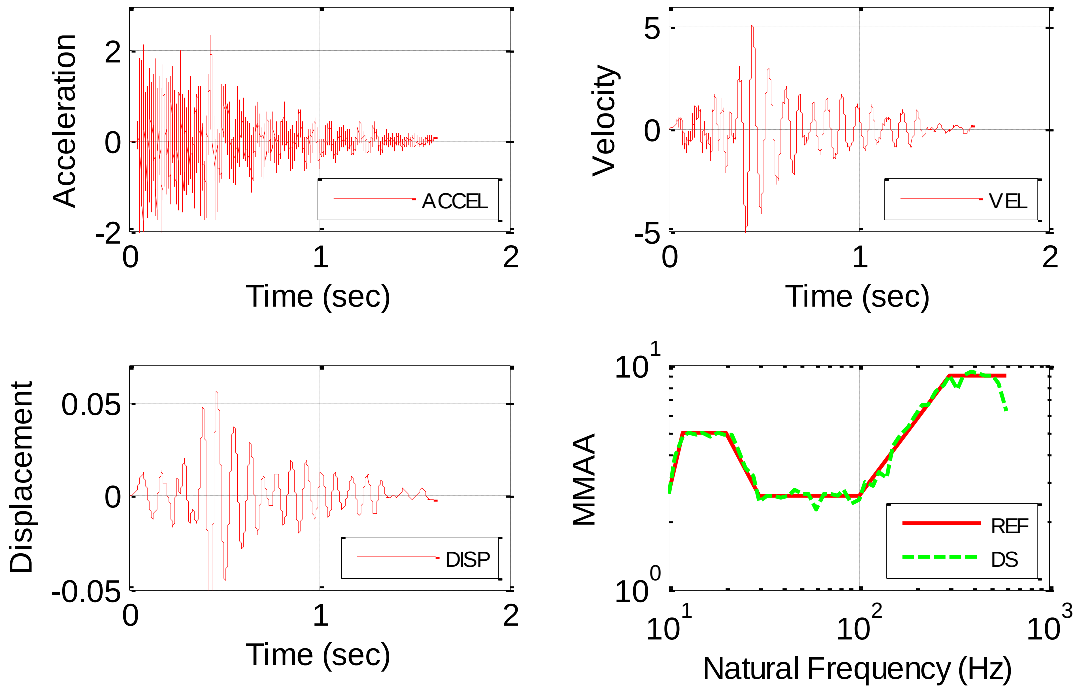

Figure 24. Decayed sine third realization.

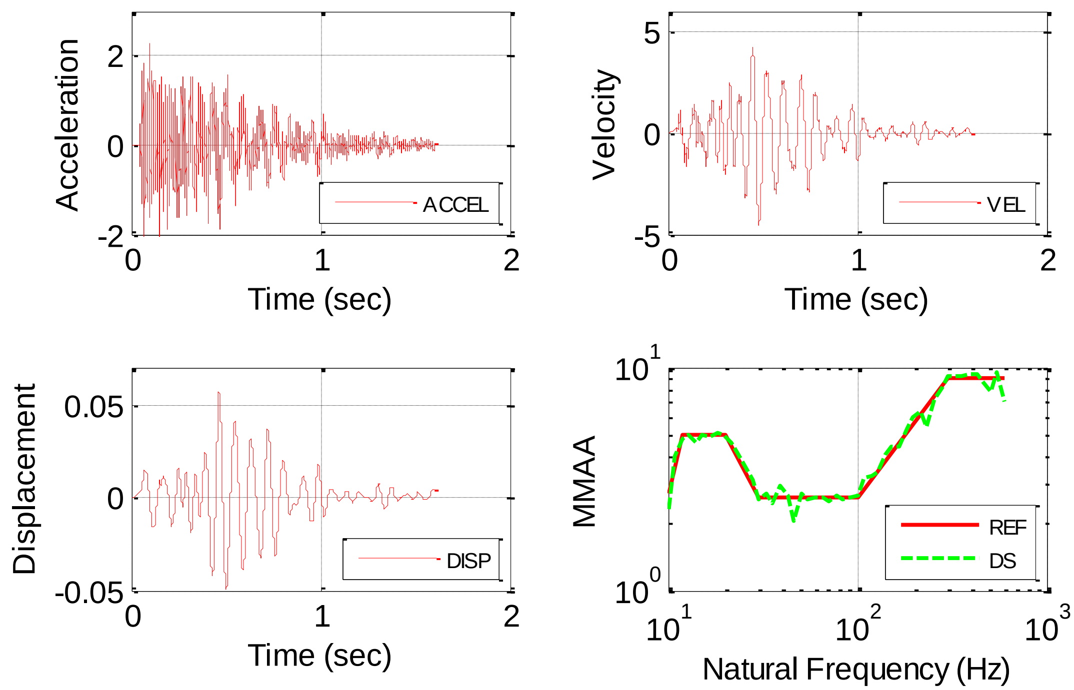

Figure 25. Decayed sine fourth realization.

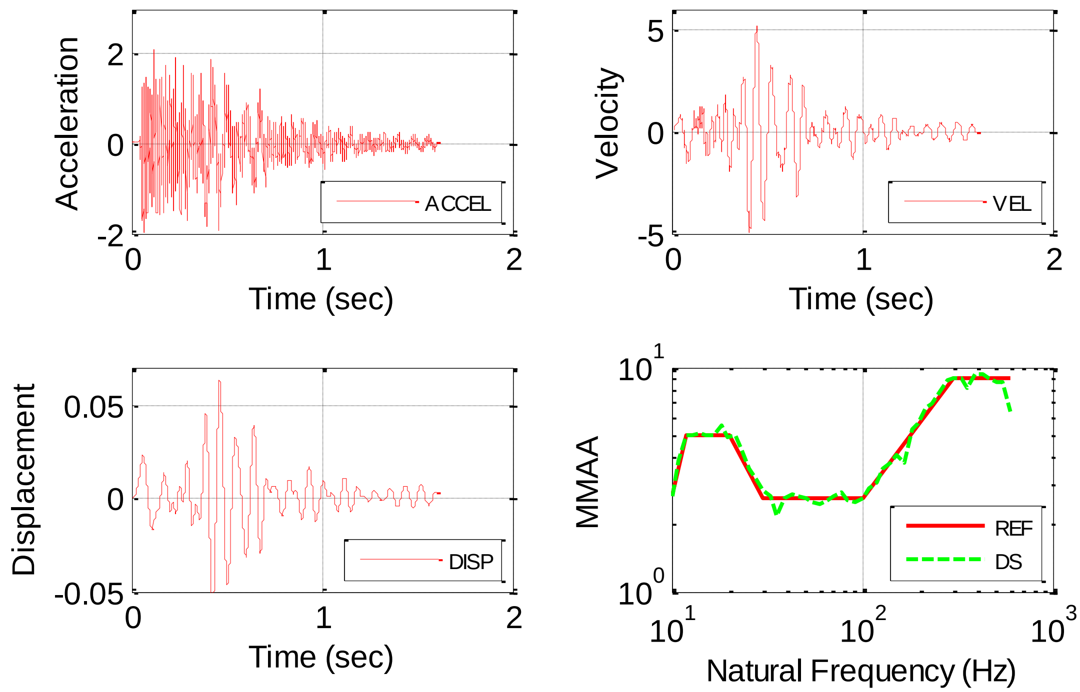

Figure 26. Decayed sine fifth realization.

6 PREVIOUS OVER-THE-ROAD TEST PROGRAMS

Note: The following describes testing where the instrumentation for measuring loads was on the transport package, not on the contents. For the current test proposal, some instruments may be placed on the external package, but the primary objective is to place instruments on the package internals – the basket, fuel assembly and fuel cladding.

6.1 "Over-the-road testing of radioactive materials packagings"[11]

Sandia National Laboratories had a program to characterize the normal environments encountered during the transport of radioactive materials. This effort consisted of obtaining experimental data from the external surface of the transport package and the transport bed during both road simulator and over-the-road tests and of analyzing the data to obtain numerical models to simulate those environments.

Test activities included 1) over-the-road testing, 2) hard braking, and 3) hard turning. Package response during any given test is specific to that package and trailer. The trailer and packaging were subjected to nine separate events to determine both the acceleration and tiedown loads experienced during normal transport. Five types of roads were used: 1) smooth asphalt primary; 2) rough asphalt primary; 3) rough concrete primary; 4) rough asphalt secondary; and 5) spalled asphalt secondary. The roads provided a vibrational environment for the packaging. To subject the packaging to a shock environment, a railroad crossing and bridge approach were selected. Finally, to determine the package's response to maneuvering, a hard turn and a stop were executed. The speed driven for each event was the lesser of either the posted legal speed limit or the fastest speed consistent with safe operation of the tractor.

For each event, approximately 15 seconds of data were recorded. This provides 15,000 samples per data channel. This was adequate time to capture shock events, such as the rail crossing plus damping back to the random vibration state. For the random vibration events, such as smooth asphalt roads, it provided a representative sampling.

[11] R.E. Glass & K.W. Gwinn, "Over-the-Road Tests of Nuclear Materials Package Response to Normal Environments," SAND91-0079, Sandia National Laboratories, December 1991.

6.1.1 Instrumentation

The primary role of the instrumentation was to obtain the acceleration at various points on the trailer and package. A total of nine instruments were used in each test. A *triaxial accelerometer* was placed on the package's center top to measure the package response along each axis. The stiffness of the package made this measurement representative of the entire package. At the same longitudinal location, an accelerometer measured the trailer's vertical acceleration. The maximum accelerations on a trailer were obtained at its front and rear. Longitudinal and vertical accelerometers were placed on the trailer bed over the rear axle, and a vertical accelerometer placed on the trailer over the kingpin. The combination of vertical accelerometer sat these three trailer locations allowed the bounce, pitch, and bending modes to be detected. The longitudinal and transverse accelerometers were useful in detecting the effects of braking and turning.

The response of the tiedown systems was determined from *load cells* in the links between attachment points and with *strain gages* mounted on the cradle straps.

6.1.2 Test results

A large volume of information is acquired from tests of this type, the actual time histories and resultant power spectral densities for each transducer. The time histories provide the mean-to-peak response at the different locations. From these time histories, the power spectral densities are generated. The power spectral densities transform the time history data into the frequency domain to relate how the response energy varies as a function of frequency. From this data, it is determined which modes of vibration are contributing to the overall response, and the root-mean square response can also be calculated. The mean squared response is the area under the power spectral densities response cue. The root mean square is the square root of this value. The root mean square relates the probability of a certain level of response occurring, and is equal to the standard deviation since the mean is zero. Three times the root mean square will envelope 99.9 percent of all expected responses. The transform magnitude plots are discrete Fourier transforms of the measured response and provide the frequency content of the transient record.

6.2 "Test specification for TRUPACT-I vibration assessment"[12]

This specification establishes the requirements for the vibration testing of a production unit Transuranic Package Transporter (TRUPACT-I). The in-service tests determined the normal transport shock and vibration environment. The purpose of the in-service tests was to determine the vibration and shock

[12] K.W. Gwinn, R.E. Glass, and L.E. Romesberg, "Test Specification for TRUPACT-I Vibration Assessment," SAND85-1369, Sandia National Laboratories, February 1986

environments encountered by the TRUPACT-I during normal service conditions. The tests will consisted of monitoring vibration and shock levels of an instrumented TRUPACT-I under normal operating conditions. The monitoring was accomplished using accelerometers located at the attachment points of the trailer.

A digital recorder was mounted on the trailer during the tests. Specific shock events of interest included railroad grade crossings, bridge approaches, potholes, raised bumps, and diagonal bumps. Vibration test events included normal primary asphaltic and concrete pavements, rough primary asphaltic and concrete surfaces, and rough secondary surfaces at a range of operating speeds. These shock and vibration events include most of the normal operating environments that would be experienced by a transport package.

6.2.1 Instrumentation

Six uniaxial piezoresistive accelerometers were attached. An accelerometer was used at each corner to measure the vertical accelerations, and the remaining two were used at the forward castings to measure longitudinal accelerations. The wiring was constrained to prevent straining during the tests. The recorder was mounted on shock isolating material to prevent recording errors and damage. All accelerometers were calibrated for a range of ±20 g.

All road simulator and over-the-road tests were instrumented to determine the loads acting on the packages. Accelerometers were used to obtain vertical, longitudinal, and transverse accelerations. Load cells were used to directly monitor tie-down loads. Strain gages were used so that tie-down loads could be calculated.

A sample of the Normal transport transducer data is given in the table below.

Peak Response for Road Surface Events

	Event				
Transducer Location	Smooth Asphalt	Rough Asphalt	Rough Concrete	Secondary Asphalt	Spalled Asphalt
Cask top					
Transverse (g)	0.17	0.21	0.12	0.13	0.22
Vertical (g)	0.23	0.32	0.20	0.35	0.58
Longitudinal (g)	0.17	0.38	0.22	0.65	0.88
Trailer, mid					
Vertical (g)	0.21	0.37	0.07	0.07	0.08
Trailer, rear					
Vertical (g)	0.46	1.4	0.95	1.68	3.1
Longitudinal (g)	0.14	0.37	0.22	0.43	0.85
Trailer, front					
Vertical (g)	0.73	1.7	1.3	2.7	4.5
Front tiedown (lb)	430	580	220	350	460
(N)	1900	2600	980	1600	2000
Rear tiedown (lb)	220	360	150	280	650
(N)	980	1600	670	1200	2900

Both peak and root mean square values that the cask response was less than 1 g.

The representative time history is shown in Figure 27 (Figure 9a) - the measured vertical acceleration of the rear trailer bed in response to the spalled asphalt event. This figure shows a fairly severe vibrational environment, with two large transient events occurring 3 and 9 seconds into the run. Figure 27 (Figure 9b) shows the same response in the frequency domain in power spectral density form. The response is shown as g^2/Hz on a log-log plot. The larger response at 1.5 Hz is due to the first bounce mode of the tractor/trailer combination. This bounce mode of the vehicle is caused by the structure bouncing in unison on the suspension system of the trailer. The next feature seen is the response at 4 Hz. This is the frequency of the vehicle's first pitching mode. This is caused by the kingpin/rear tractor suspension deflecting down while the trailer rear suspension and tractor front suspension deflect up. The high-frequency modes, from 10 to 20 Hz, are combinations of the trailer bending with the tractor pitching and bending. The first bending mode occurs at approximately 11 Hz.

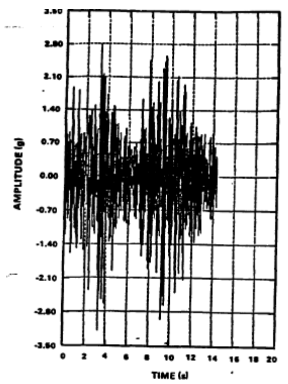

Figure 9a. Representative Time History

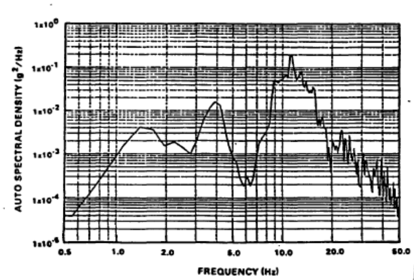

Figure 9b. Representative PSD

Figure 27. Representative normal transport load data.

7 KEY BACKGROUND INFORMATION

7.1 Souce of Vibration and Shock Data for Test

EDB #A2164

EXTRACTED FROM

SAND77-1110
Unlimited Release
Printed September 1977

NRC-12

SHOCK AND VIBRATION ENVIRONMENTS FOR LARGE SHIPPING CONTAINER DURING TRUCK TRANSPORT (PART I)

Cliff F. Magnuson
Applied Mechanics Division II 1282
Sandia Laboratories, Albuquerque, NM 87115

[3]

ABSTRACT

The purpose of this study was to obtain vibration and shock data during truck shipment of heavy cargo. Currently available data were taken on trucks bearing lighter loads than the loads of current interest. In addition, the new data are expected to be useful in the determination of any trends of vibration and shock environments with increased cargo weight. These new data were obtained on a "piggyback" basis during truck transport of 195 700 N (44,000 lb) cargo which consisted of a spent fuel container and its supporting structure from Mercury, Nevada, to Albuquerque, New Mexico. The routes traveled were US 95 from Mercury, Nevada, to Las Vegas, Nevada; US 93 from Las Vegas to Kingman, Arizona; and I-40/US 66 from Kingman to Albuquerque, New Mexico. Speeds varied from very slow during hill climbs to 101 km/hr (63 mph). A comparison of these data with a collectively reduced set of data for cargo weights varying from no-load to 133 400 N (30,000 lb) showed that the zero to peak amplitude levels of vibration were significantly lower for frequencies less than 40 Hz in the vertical axis and that there was a reduction in the vibration amplitude levels in all axes for frequencies greater than 500 Hz. The shock response amplitude was less severe for the entire frequency spectrum in the vertical axis, but it was not significantly different in the other axes. Data measurements were made on a truck shipment of a 249 100 N (56,000 lb) container over the same routes as were used for the shipment discussed in this report. These data will be presented in a subsequent report along with any additional data trends that result from studies of trucks carrying increased cargo weight.

EDB #A2165
EXTRACTED FROM

NUREG/CR-0128
SAND78-0337
RT

SHOCK AND VIBRATION ENVIRONMENTS FOR A LARGE SHIPPING CONTAINER DURING TRUCK TRANSPORT (PART II)

Clifford F. Magnuson

Manuscript Submitted: February 13, 1978
Date Published: May 1978

[2]

Manuscript Submitted: February 13, 1978
Date Published: May 1978

Sandia Laboratories
Albuquerque, New Mexico 87185
operated by
Sandia Corporation
for the
U.S. Department of Energy

Prepared for
Division of Safeguards, Fuel Cycle and Environmental Research
Office of Nuclear Regulatory Research
U.S. Nuclear Regulatory Commission
Washington, DC 20555
Under Interagency Agreement DOE 40-550-75
NRC FIN No. A-1049-6

ABSTRACT

The purpose of this study was to obtain vibration and shock data during truck shipment of heavy cargo. These data were for use in determining any trends of vibration and shock environments with increased cargo weight. The new data were obtained on a "piggyback" basis during truck transport of 249 100N (56,000-pound) cargo which consisted of a spent fuel container and its supporting structure. The truck was driven from Mercury, Nevada, to Albuquerque, New Mexico. The routes traveled were US 95 from Mercury, Nevada, to Las Vegas, Nevada; US 93 from Las Vegas to Kingman, Arizona; and I-40/US 66 from Kingman to Albuquerque, New Mexico. Speeds varied from very slow to 88 km/hr (55 mph). A comparison of data from similar experiments with cargo weights varying from no-load to this load shows that the zero-to-peak acceleration amplitude levels of vibration are highest when trucks carry relatively light loads. This is true for the longitudinal and vertical axes of the vehicles in most frequency bands and for the transverse axis above 700 Hz. The shock response acceleration amplitudes for heavier cargo weights were less severe above 3 Hz in the vertical axis and higher between 8 and 20 Hz in the transverse axis. The highest acceleration amplitude of shock response in the longitudinal axis below about 20 Hz was produced in a trailer having a spring suspension system and carrying the 249 100N (56,000 pounds) load.

7.2 Related Documents

7.2.1 "Approach for the Use of Acceleration Values for Packages of Radioactive Material under Routine Conditions of Transport," Andreas Apel, Viktor Ballheimer, Christian Kuschke, Sven Schubert, Frank Wille, Proceedings of the 9th International Conference on the Radioactive Materials Transport and Storage, May 2012, London.

7.2.2 "Transportation Activities for BWR Fuels at NFI," S. Uchikawa, H. Kishita, H. Ide, M. Owaki, K. Ohira, Nuclear Fuel Industries, LTD., Proceedings of Global 2009, Paris, September 2009.

Nuclear Fuel Industries, LTD. (NFI) supplies fuel assemblies for both PWR and BWR nuclear power plants in Japan. We also are involved in the field of nuclear fuel recycling and we manage transportation of the fuel assemblies from our fabrication facilities to the Japanese nuclear power plants. The NT-XII transportation container was developed by NFI for fresh BWR fuel assemblies. The foremost design priorities for this NT-XII container were transportation efficiency and ensuring fuel integrity during transportation. In addition to the design of new containers, we also develop improved packaging methods. Recently, NFI performed tests intended to determine the need for packing separators to mitigate vibration induced wear during fuel transportation. The transportation test was performed using dummy fuel assemblies and included wear data analysis and post-disassembly inspections. The fretting wear on the surface of fuel rods and spacer spring force degradation were measured. Results from these evaluations indicated that there was no significant difference in the vibration induced wear on the fuel between the packaging methods with and without packing separators. As a result, NFI developed a new packaging method which improves the packing and unpacking efficiency for fuel rods transported from the fuel fabrication facility to another facility. This method also enables the fuel assembly container to be used without the need for modifications to the design of container.

7.2.3 "High Burn-up Used Nuclear Fuel Vibration Integrity Study - Out-of-Cell Fatigue Testing Development,", Jy-An John Wang, Hong Wang, Yong Yan, Rob Howard, Bruce Bevard, January 2011, Oak Ridge National Laboratory.

For high burn-up spent nuclear fuel (SNF), it is expected that the used nuclear fuel cladding will have a high population of microcracks and hydrides, including macro-hydrides and micro-hydrides. This will reduce the stress intensity required to advance the crack growth. The linking of these microcracks during vibration loading may also reduce the fatigue threshold/incubation period, accelerating fatigue failure. In addition to the cladding damage, the microstructure of comprising fuel pellets and the interfaces of fuel rod have changed dramatically after high burn-up in the reactor. These changes may have a direct impact on the structural integrity and vibration response of SNF rods in transportation.

As a result, vibration has been included as a mandatory test condition for the structural evaluation of package that is used in transporting spent nuclear fuel by US NRC (Nuclear Regulatory Commission) in 10 CFR §71.71. Currently, no testing system is available to test the spent nuclear fuel and evaluate the performance of fuel rods during transportation. It is the aim of this research project to develop a system that can appropriately test the response of high burn-up SNF rods under simulated loading conditions.

The SNF rods lie horizontally in a transportation cask and are supported by the spacers within fuel rod assembly. These rods are subjected to oscillatory bending due to inertia effects. This oscillatory bending is the major vibrational load of SNF rods as mentioned in 10 CFR §71.71 and its effect on integrity of the SNF rods needs to be captured by the designed testing system. The SNF rods include various burn-induced damage (pores and micro cracks), oxide and hydride layers, residual stresses, altered interfaces, and trapped fission products. They are highly radioactive. These factors complicate conventional cyclic bending testing and need to be considered in the development of the test apparatus.

An extensive literature survey revealed that a variety of bending fatigue testing methods have been developed including cantilever beam bending, three-point/ four-point bending, and pure bending, as well as their variants considering environmental factors, particularly temperature. Bending fatigue testing approaches also account for rotation based on if the rotation is introduced to carry out the reverse bending. However, the vibration of SNF rods during transportation usually involves deflection instead of rotation, and at the same time, the dominant frequencies involved with these dynamical events are generally less than 100 Hz. Therefore, the non-rotating reverse bending that can be accomplished by a universal material testing machine or its equivalent is the focus of this report.

Currently, bending cyclic fatigue test methods are used in testing and characterizing various engineering materials and their components including concrete, composites, ceramics, metal alloys, metallic glasses, and so forth. Available approaches include unipolar mode without reversal, and bipolar mode with full reversal. Mechanical support/ contact techniques to enable the designed beam bending boundary condition have been advanced significantly. But most of the bending fatigue tests are application-based. The following conclusions can be drawn from the literature survey:

- Among the bending fatigue testing methods reviewed, four-point bending fatigue testing is a mature experimental technology in testing materials and components that have a limited deformation before failure. Demonstration of this technology includes asphalt beam and the development of a self-aligning test rig.
- The above-mentioned techniques are mainly used in fatigue tests without bending reversal.
- A variety of supports were developed in bending fatigue testing including rotary joints, slide connection, and flexures. They either deviate from a true fixed boundary condition or involve contact damage.
- Four-point/ three-point bending and cantilever bending all suffer from an inherent drawback related to shear in the beam that has a non-uniform bending moment. This has a significant impact on testing materials that are sensitive to the shear.
- Pure bending fatigue has been used for high strain fatigue testing of metal alloys and composites. The implementation of the pure bending concept is application-based and has been partially successful.
- Environmental chambers and/or high temperature furnaces are currently incorporated into some critical bending fatigue tests. Specimen setup is usually manual and therefore insufficient for testing materials that are radioactive.

A bending fatigue testing system has been proposed and developed in this report to test high burn-up SNF rods. Pure bending is adopted as the bending mode of testing system. The use of a pure bending method in which a uniform bending moment is exerted on the gage length of the specimen should eliminate the effect of shear. The shear can eventually lead to a failure mode that is not relevant to the fatigue failure of concern. Two implementation concepts are presented with emphasis on bending fatigue testing on rod specimens in reversal bending.

The first implementation relates to an approach in which the specimen is setup horizontally. Some important features are

- It is based on the principle of four-point bending, but the gage length of the specimen is arranged in the part of beam that has a uniform bending moment. The driving mechanisms in conventional four-point testing can be applied to the horizontal setup.
- Rigid sleeves are introduced to reinforce the extensional parts of specimen and to convert external force couples into the bending moments.
- It accommodates various connections to loading contacts and supports. These connection options enable the free rotation and horizontal translation of beam boundary condition as required by reversal bending and can best fit into the different applications.

The second implementation concerns the design with the specimen setup vertically. The main features are

- Bending moments are applied through two horizontal rigid arms of a U-frame structure. The arms are equipped with two co-axial holes that accommodate the test specimen.
- Roller bearings or equivalent bearing sets in the arms of the U-frame allow the release of any axial load related to the loading of specimen and, at the same time, transfer the bending moments from the rigid arms to the specimen.
- The initial setup of a test specimen can be accomplished by a simple insertion of the specimen into the holes. This is advantageous for a hot-cell environment because most of the operations can be adapted for this testing environment.
- The U-frame has fewer components, which would result in a test system with enhanced reliability and controllability.
- Versatile designs in the vertical member and joints or corners of the U-frame provide options for different experimental studies.

Overall, the proposed test system has the following unique characteristics in comparison with the conventional bending fatigue testing methods:

- Bending fatigue testing is carried out under pure bending, eliminating the effect of the shearing force encountered in three-point bend and four-point bend testing.
- The bending fatigue is conducted in a reversal mode and the system approaches the loading condition of used nuclear fuel in transportation more closely than repeated three-point or four-point bending testing.
- Compliant layers are incorporated into the rigid sleeve to control the effect of contact on the fatigue failure in the specimen retaining areas.

- The system can test and examine specimens in very hostile or radioactive environments.

7.2.4 Other documents related to this work include

7.2.4.1 "Mechanical Behaviour of High Burn-Up SNF under Normal and Accident Transport Conditions – Present Approaches and Perspectives," Fanke Wille, Viktor Ballheimer, Annette Rolle, Berhard Droste, Bundesanstalt für Materialforschung und –prüfung (BAM).

7.2.4.2 "CANDU Irradiated Fuel Transportation: The Shock and Vibration Program," B.P. Dalziel, M.A. Elbestawi, J.W. Forest, Ontario Hydro, Research Agreement Report No. 2715/R1/CF.

7.2.4.3 "Transportation Shock and Vibration Descriptions for Package Designers," J.T. Foley, Sandia National Laboratories Report SC-M-72 0076, July 1972.

7.2.4.4 "Design Basis for Resistance to Shock and Vibration," SAND89-0937C, R.E. Glass, K.W. Gwinn, Sandia National Laboratories.

7.2.4.5 "Over-the-Road Testing of Radioactive Materials Packaging" SAND91-2709C, R.E. Glass and K.W. Gwinn, Sandia National Laboratories.

8 REFERENCES

[1] "A Method for Determining the Spent-Fuel Contribution to Transport Cask Containment Requirements," Thomas L. Sanders, Kevin D. Seager, Sandia National Laboratories; Yusef R. Rashid, Peter R. Barrett, ANATECH Research Corporation; Anthony P. Malinauskas, Oak Ridge National Laboratory; Robert E. Einziger, Pacific Northwest Laboratory; Hans Jordan, EG&G Rocky Flats Inc.; Thomas A. Duffey, Stephen H. Sutherland, APTEK Incorporated; Philip C. Reardon, GRAM Incorporated, SAND90-2406, November 1992.

[2] "Shock and Vibration Environments for a Large Shipping Container during Truck Transport (Part II)," Clifford F. Magnuson, Extracted from NUREG/CR-0128, SAND78-0337, Sandia National Laboratories, May 1978.

[3] "Shock and Vibration Environments for a Large Shipping Container during Truck Transport (Part I), Clifford F. Magnuson, SAND77-1110, Sandia National Laboratories, September 1977.

[4] "Shock and Vibration Environments Encountered During Normal Rail Transportation of Highway Cargo," Magnuson, C.F., Sandia National Laboratories, Albuquerque, NM, SAND82-0819, August 1982.

[5] "Shock Environments for Large Transport Containers during Rail-Coupling Operations," Magnuson, C.F., Sandia National Laboratories, Albuquerque, NM, SAND79-2168, NUREG/CR-1277, June 1980.

[6] US Code of Federal Regulations, Title 10-Energy, Party 71 (10 CFR 71), "Packaging and Transportation of Radioactive Material."

[7] "Standard Review Plan for Transportation Packages for Radioactive Material," NUREG-1609, US Nuclear Regulatory Commission, March 1999.

[8] "Dynamic Analysis to Establish Normal Shock and Vibration of Radioactive Material Shipping Packages, Volumes 1-3," S.R. Fields, NUREG/CR-2146, US Nuclear Regulatory Commission, 1983.